Sulindac modulates secreted protein expression from LIM1215 colon carcinoma cells prior to apoptosis

David W. Greening[1], Hong Ji[1], Eugene A. Kapp[2] and Richard J. Simpson[1*]

[1] *La Trobe Institute for Molecular Science (LIMS), La Trobe University, Bundoora, Victoria, Australia*

[2] *Bioinformatics Division, Walter & Eliza Hall Institute of Medical Research, Parkville, Victoria, Australia*

**Corresponding author*

Prof. Richard J. Simpson

La Trobe Institute for Molecular Science (LIMS)

La Trobe University

Bundoora, Victoria, 3083 Australia

Fax: +61 3 9479 1266

Email: Richard.Simpson@latrobe.edu.au

Keywords: sulindac, secretome, colon cancer, NSAIDs, chemoprevention, peptidome

ABBREVIATIONS

CM, culture medium

COX, cyclooxygenase

CRC, colorectal cancer

ECM, extracellular matrix

FA, focal adhesion

FAK, focal adhesion kinase

HNPCC, Hereditary nonpolyposis colorectal cancer

MSI, microsatellite instable

MMP, Matrix metalloproteinase

MSS, microsatellite stable

MTT, 3-(4,5-dimethylthiazol-2-yl)-2,5-diphenyltetrazolium bromide

NMWC, nominal molecular weight cut-off

N_{SC}, normalized spectral count

NSAID, nonsteroidal anti-inflammatory drug

PI, propidium iodide

PS, phosphatidylserine

RIP, regulated intramembrane proteolysis

R_{SC}, spectral count fold change ratio

SFM, serum-free media

SUMMARY

Colorectal cancer (CRC) is a major cause of mortality in Western populations. Growing evidence from human and rodent studies indicate that nonsteroidal anti-inflammatory drugs (NSAIDs) cause regression of existing colon tumors and act as effective chemopreventive agents in sporadic colon tumor formation. Although much is known about the action of the NSAID sulindac, especially its role in inducing apoptosis, mechanisms underlying these effects is poorly understood. In previous secretome-based proteomic studies using 2D-DIGE/MS and cytokine arrays we identified over 150 proteins released from the CRC cell line LIM1215 whose expression levels were dysregulated by treatment with 1 mM sulindac over 16 h; many of these proteins are implicated in molecular and cellular functions such as cell proliferation, differentiation, adhesion, angiogenesis and apoptosis (Ji et al., *Proteomics Clin. Appl*. 2009, 3, 433-451). We have extended these studies and describe here an improved protein/peptide separation strategy that facilitated the identification of 987 proteins and peptides released from LIM1215 cells following 1 mM sulindac treatment for 8 h preceding the onset of apoptosis. This peptidome separation strategy involved fractional centrifugal ultrafiltration of concentrated cell culture media (CM) using nominal molecular weight membrane filters (NMWL 30K, 3K and 1K). Proteins isolated in the >30K and 3-30K fractions were electrophoretically separated by SDS-PAGE and endogenous peptides in the 1-3K membrane filter were fractioned by RP-HPLC; isolated proteins and peptides were identified by nanoLC-MS-MS. Collectively, our data show that LIM1215 cells treated with 1 mM sulindac for 8 h secrete decreased levels of proteins associated with extracellular matrix remodeling (e.g., collagens, perlecan, syndecans, filamins, dyneins, metalloproteinases and endopeptidases), cell adhesion (e.g., cadherins, integrins, laminins) and mucosal maintenance (*e.g.*, glycoprotein 340 and mucins 5AC, 6, and 13). A salient finding of this study was the increased proteolysis of cell surface proteins following treatment with sulindac for 8 h (40% higher than from untreated LIM1215 cells); several of these endogenous peptides contained C-terminal amino acids from transmembrane domains indicative of regulated intramembrane proteolysis

(RIP). Taken together these results indicate that during the early-stage onset of sulindac-induced apoptosis (evidenced by increased annexin V binding, dephosphorylation of focal adhesion kinase (FAK), and cleavage of caspase-3) 1 mM sulindac treatment of LIM1215 cells results in decreased expression of secreted proteins implicated in ECM remodeling, mucosal maintenance and cell-cell-adhesion.

INTRODUCTION

Colorectal cancer (CRC) is the second leading cause of cancer death in Western populations, with more than a million new cases and half a million deaths worldwide annually [1]. One of the most widely studied and promising chemopreventive agents for sporadic CRC [2] and therapeutic agent for the treatment of adenomas in patients with familial adenomatous polyposis (FAP) [3] is the non-steroidal anti-inflammatory drug (NSAID) sulindac; for a review see [4, 5]. While epidemiological evidence indicates that continued use of NSAIDs such as aspirin is associated with reduced risk of CRC in the general population [6], animal (rodent) data for aspirin is less conclusive [7]. However, the potential harms associated with the chronic use of NSAIDs such as gastrointestinal and cardiovascular complications are well documented [8-10] and warrant careful consideration before adoption for general clinical use. Investigation of mechanisms associated with antineoplastic effects of NSAIDs may provide insight that could lead to new drug candidates that are potentially safer and more efficacious for CRC chemoprevention.

The chemopreventive effects of NSAIDs occur primarily through inhibition of the cyclooxygenase-(COX)-1 and COX-2 enzymes [11, 12], which are involved in the synthesis of prostaglandins leading to a decreased activation of the inflammatory response [13], inhibition of crypt cell proliferation [14], angiogenesis [15] and increased apoptosis [16]. At the molecular level NSAIDs are also reported to target a number of COX-independent cellular processes, including peroxisome proliferator-activated receptor (PPAR) subtypes γ and δ, nuclear factor-κB (NF-κB) pathway, and the multidrug-resistance protein 4 (MRP4) [17]. The mechanism(s) by which sulindac prevents CRC are complex and poorly understood, especially in the early-onset stage of apoptosis; for a review of the role of NSAIDs in CRC progression and underlying mechanisms of action, see Antonakopoulos and Karamanolis [18].

Although our understanding of cancer cell biology has advanced considerably [19], there is, however, a growing awareness that targeting the cancer cell in isolation is not sufficient because of the intricate reciprocal interplay between cancer cells and the tumor microenvironment [20, 21]. In addition to epithelial tumor cells, the microenvironment consists of several non-malignant, albeit genetically altered, heterotypic cell types (e.g., fibroblasts, endothelial cells and leukocytes) which crosstalk either physically or via secretion (collectively referred to as the secretome) of paracrine signaling molecules [22]. As well as cytokines, chemokines, growth factors, proteases and protease inhibitors, the secretome also contains extracellular vesicles [23]. It is now recognized that pathophysiology of the tumor microenvironment is critical for neoplastic induction and progression and is now a primary target for cancer chemoprevention [24, 25]. While most proteomics-based studies on NSAID action have focused on cellular proteins, systematic analyses of proteins released from CRC cells into the tumor microenvironment - in response to NSAID treatment are limited [26].

As a first step towards understanding the molecular events associated with the chemopreventive action of the NSAID sulindac in the context of the tumour environment, we have employed the human colon carcinoma cell line LIM1215 to assess the early effects of sulindac (i.e., prior to onset of apoptosis) on secretome protein expression levels. This study focuses on identifying secreted modulators involved in sulindac-mediated apoptosis in CRC adenomas. Specifically, we have employed two different proteomic analyses; a bottom-up approach (focused on characterising secreted proteins) and a top-down approach (focused on characterising low-M_r secreted polypeptides). It is anticipated that this approach will improve our understanding of the extracellular contribution to the chemopreventive effects of sulindac on CRC and provide the foundation for improved chemopreventive target design.

EXPERIMENTAL PROCEDURES

Cell culture and reagents - The human colon carcinoma cell line LIM1215 [27] was routinely cultured on 150-mm diameter cell culture dishes (2×10^6 cells/dish) in RPMI-1640 medium (Invitrogen, Carlsbad, CA) supplemented with 5% FCS (CSL, Melbourne), 100 U penicillin and 100 mg/mL streptomycin (Sigma-Aldrich), and incubated at 37 °C in a humidified atmosphere containing 10% CO_2 until sub-confluent (80-90%). RPMI-1640 medium containing with sulindac (0.2-1 mM), was prepared fresh by adding appropriate aliquots of a 1 M stock solution of sulindac (Sigma-Aldrich) reconstituted in 1.5 M Tris-HCl, pH 8.5. For control studies an identical volume of 1.5 M Tris-HCl, pH 8.5 buffer was combined with RPMI-1640 media. Cell proliferation and viability assays were performed using 3-(4,5-dimethylthiazol-2-yl)-2,5-diphenyltetrazolium bromide (MTT) absorbance at 595 nm and Trypan Blue dye exclusion assays, respectively.

Annexin V binding assay - Apoptosis was evaluated using TACS™ (Trevigen Apoptotic Cell System) Annexin V kit (Trevigen, Gaithersburg, MD). Cells were treated with either vehicle alone (1.5 mM Tris-HCl, pH 8.5) or 1 mM sulindac for time periods of 2, 4, 6 and 8 h and washed with ice-cold PBS, followed by incubation with Annexin V-FITC Incubation Reagent for 15 min. Following incubation cells were washed twice with excess 1 × Binding Buffer and viewed using an Olympus FV1000 confocal system attached to an Olympus IX81 microscope (Olympus, Tokyo, Japan).

Live cell imaging - LIM1215 cells were cultured in RPMI-1640 medium containing 5% FCS in an 8-well Ibidi µ-Slide (Ibidi, Munich, Germany) for 24 h until cell density reached ~80% confluency. Cells were washed 4 × with phenol red free RPMI-1640 medium and treated with 1 mM sulindac in RPMI medium containing propidium iodide (PI). Immediately following treatment, live cell imaging was performed, with cells maintained in 5% CO_2 at 37 °C by a custom-built incubator and controller (Clear State Solutions, Australia). Cells were imaged every 20 min for 24 h on an Olympus FV1000 confocal system attached to an Olympus IX81 microscope, using a UPlanSApo 0.9 numerical aperture (NA)/40× objective. Excitation was supplied via a 635 nm laser and captured by the transmitted light detector of the system. The resulting time series was analyses and movies created using MetaMoprh v7.6.3 (Molecular Devices, USA).

Immunofluorescence staining and microscopy - For immunofluorescence staining, LIM1215 cells were cultured in serum containing RPMI medium in an 8-well Ibidi µ-Slide (Ibidi) until cell density reached ~80% confluency. Cells were washed 4 × with RPMI-1640 medium and treated with 1 mM sulindac in RPMI medium for defined time periods at 37 °C. Following each treatment, cells were washed twice with ice-cold PBS, fixed for 10 min in 3.7% formaldehyde, washed twice with PBS, permeabilized in 0.2% TX-100 in PBS for 5min, washed twice with PBS and blocked for 30 min (0.5% BSA, 5% normal goat serum and 0.1% gold fish skin gelatin in PBS). Fluorescent-labeled primary mouse anti-laminin-γ1 (Abcam) (1:200) or mouse anti-E-cadherin (BD Biosciences, Franklin Lakes, NJ) (1:500) antibodies were used, followed by secondary Alexa 568-conjugated goat anti-mouse antibody labeling (Invitrogen). Nuclei were counterstained using DAPI (Invitrogen) at 300 nM. Cells were imaged using a Nikon ECLIPSE TE2000-E confocal microscope equipped with a Nikon plan APO VC 60x/1.20 WI water-immersion lens.

Whole cell lysate (WCL) preparation – One plate of 80% confluent cells was washed twice with ice-cold PBS (10 mL) and lysed with 2 mL of 2 × SDS sample buffer (4% (w/v) SDS, 20% (v/v) glycerol and 0.01% (v/v) bromophenol blue, 0.125 M Tris-HCl, pH 6.8) for 10 min on ice, followed by centrifugation (400,000 × g, 30 min) (TLA-100.2 rotor, Beckman) to remove insoluble material. Supernatants were collected, and stored at -80 °C for subsequent use.

Secretome preparation - For preparation of the soluble-secretome (*i.e.*, no membrane vesicles), sub-confluent LIM1215 adherent cells were washed 4 × in RPMI-1640 media and cultured in serum-free RPMI-1640 media, in presence and absence of 1 mM sulindac, for 8 h. Following treatment, culture media (CM) from both sulindac-treated and control cell cultures were harvested by centrifugation at 480 × g for 5 min to sediment non-adherent cells, and the supernatant further centrifuged at 2000 × g for 10 min at 4 °C to remove cellular debris. Complete EDTA-free Protease inhibitor cocktail tablets (Roche) were immediately dissolved in the resultant supernatants. Each supernatant (~150 mL) was filtered through separate VacuCap® 60 filter units (Pall Life Sciences) with 0.1 µm Supor® to remove suspended cells and membrane vesicles and placed on ice. Ultracentrifugation was performed at 100,000 × g at 4 °C for 2 h (Beckman Coulter Optima MAX Ultracentrifuge) to obtain CM supernatants.

Differential centrifugal ultrafiltration - CM supernatants from each cell line were fractionated through a series of Amicon® Ultra-15 (Millipore) and Macrosep® Omega (Pall Life Sciences) centrifugal filter devices as described (Greening, *manuscript submitted*). Membranes were pre-rinsed with deionized water (A10-Synthesis™ water polishing system, Millipore), and subsequently RPMI-1640 medium. CM supernatants were filtered initially through Amicon® Ultra-15 30,000 nominal molecular weight limit (NMWL) centrifugal filter devices (3,000 × g, 4 °C), with each filtrate (flow-through, <30K) subsequently filtered through an Amicon® Ultra-15 3,000 NMWL filter (3,000 × g, 4 °C). Filtrates (flow-through, <3kDa) were concentrated to ~2 mL using a 1,000 NMWL Macrosep® Omega centrifugal device (2,500 × g, 4 °C), to obtain the secretopeptidome (1-3K fractions) [28]. Therefore, from each CM supernatant fractions (i) >30K, (ii) 3-30K, and (iii) 1-3K were obtained. Centrifugation conditions were optimized as previously described [28-30] to ensure 95% (v/v/) filtrate recovery.

Protein quantitation - The protein content of secretome fractions and WCL preparations was estimated by 1D-SDS-PAGE / SYPRO® Ruby protein staining / densitometry [31]. Briefly, 5 µL sample aliquots were solubilized in SDS sample buffer (2% (w/v) sodium dodecyl sulfate, 125 mM Tris-HCl, pH 6.8, 12.5% (v/v) glycerol, 0.02% (w/v) bromophenol blue) and loaded into 1 mm, 10-well NuPAGE™ 4-12% (w/v) Bis-Tris Precast gels (Invitrogen). Electrophoresis was performed at 150 V for 1 h in NuPAGE™ 1 × MES running buffer (Invitrogen) using an Xcell Surelock™ gel tank (Invitrogen). After electrophoresis, gels were removed from the tank and fixed in 50 mL fixing solution (40% (v/v) methanol, 10% (v/v) acetic acid in water) for 30 min on an orbital shaker and stained with 30 mL SYPRO® Ruby (Life Technologies, NY, USA) for 30 min, followed by destaining twice in 50 mL of 10% (v/v) methanol with 6% (v/v) acetic acid in water for 1 h. Gels were imaged on a Typhoon 9410 variable mode imager (Molecular Dynamics), using a green (532 nm) excitation laser and a 610BP30 emission filter at 100 µm resolution. Densitometry quantitation was performed using ImageQuant software (Molecular Dynamics) to determine protein concentration relative to a BenchMark™ Protein Ladder standard of known protein concentration (Invitrogen). Protein concentrations of 1-3K fractions were determined by absorbance at A280 nm using ND-2000 spectrophotometer (NanoDrop, USA).

Analytical RP-HPLC fractionation - Analytical RP-HPLC of 1-3K fractions were performed using an 1100 HPLC system (Agilent Technologies), with column eluent monitored using a diode-array detector fitted with a standard 13-µL flow-cell (Agilent Model G1315B) and a multi-wavelength fluorescent detector fitted with a standard 8-μL flow-cell (Agilent Model G1321A) coupled in-line. Peptidome fractions (1-3K, 100 μg, 0.5 mL) were manually injected (2 mL sample loop) onto a Brownlee Aquapore RP-300 cartridge (100 × 2.1 mm id, octylsilica 300Å pore size, 7 μm dp (Perkin-Elmer)). Sample injections were made up with 1:1 solvent A, 0.1% (v/v/) aqueous TFA. The column was developed at 100 μL/min over 75 min at room temperature using a linear 60-min gradient from 0–100% solvent B; 0.1% aqueous TFA, 60% CH_3CN. Column eluent was monitored for UV absorbance at 215 nm. 100 μL fractions were collected (t = 14-50 min) into 96-well low-protein binding plates (Agilent Technologies), after correcting for the post-column dead volume (50 μL). Fractions were concentrated to ~20 μL by centrifugal lyophilisation (SpeedVac AES 1010, Savant, U.S.A.) prior to sample injection for nanoLC-MS/MS analysis.

1D SDS-PAGE, gel *excision, reduction, alkylation, and trypsinisation* – For secretome >30K and 3-30K fractions, 30 μg were electrophoresed on a NuPAGE® Novex 4-12% Bis-Tris Gel (Invitrogen). Electrophoresis was performed at constant 150 V in NuPAGE® MES Running Buffer (Invitrogen) for 50 min. Proteins were visualized using Imperial Protein Stain (Pierce, Rockford, IL) according to manufacturer’s instructions. 23 × 1.5-mm gel bands were excised from each gel lane and individual bands subjected to automated in-gel reduction, alkylation, and tryptic digestion [32] using the MassPREP® Robotic Liquid Handling Station (Micromass). Briefly, gel sections were reduced with 10 mM DTT (Calbiochem) for 30 min, alkylated for 20 min with 25 mM iodoacetic acid (Fluka), and digested with 150 ng trypsin (Worthington, Lakewood, NJ) for 4.5 h at 37 °C. Extracted peptide solutions for each fraction were concentrated to ~10 μL by centrifugal lyophilisation using a SpeedVac AES 1010 (Savant) for subsequent LC-MS/MS analysis.

nanoLC-MS/MS – NanoLC-MS/MS experiments were performed with a 1200 series nanoLC system (Agilent) equipped with a UPLC nano-Acquity® C18 150 × 0.15 mm i.d. column (Waters, Milford, MA). The system was developed with a linear 60-min gradient with a flow rate of 0.8 μL/min at 45 °C from 0-100% solvent B, where solvent A was 0.1% aqueous formic acid and solvent B was 0.1% aqueous formic acid/60% CH_3CN. The nanoHPLC was coupled on-line to an LTQ-Orbitrap mass spectrometer equipped with a nanoelectrospray ion source (Thermo Fisher Scientific) for automated MS/MS, as described [30, 33]. All collected and lyophilised fractions for 1-3K samples, and trypsinised fractions for >30K and 3-30K fractions were analyzed.

Database searching and bioinformatic analysis - Peak lists were extracted using the Extract-MSn program as part of Bioworks 3.3.1 (Thermo Fisher Scientific). Parameters used to generate peak lists were as follows: minimum mass 700, maximum mass 7000, grouping tolerance 0.001 Da, minimum group count 1, 10 peaks minimum and total ion current of 100. Peak lists for each LC-MS/MS run were merged into a single Mascot generic file (MGF) for Mascot searches. Automatic charge state recognition was used because of the high-resolution survey scan (30,000). MGF files were searched using the Mascot v2.3.01 search algorithm (Matrix Science) against the Q112 LudwigNR protein sequence database with a taxonomy filter for human comprising 137 881 entries (http://www.ludwig.edu.au/archive/LudwigNR/LudwigNR.pdf). The search parameters were as follows: Peptidome (1-3K) unrestricted search (no-enzyme) with N-terminal protein acetylation as variable modification. For 3-30K and >30K, trypsin used with two missed cleavages, carboxymethylation of cysteine as a fixed modification (+58 Da), N-terminal acetylation (+42 Da) and methionine oxidation (+16 Da) simultaneously allowed as variable modifications. A peptide mass tolerance of ±30 ppm, #13C defined as 1, and fragment ion mass tolerance of ±0.7 Da was used. The automatic decoy (random) database sequence option was enabled to allow false-discovery rate estimation. The program *MSPro*, previously described [28, 34], was used for collating all Mascot search result files and extracting all peptide identifications. All peptides from target and decoy searches scoring ≥ 13 (Mascot Ionscore) were passed to the post-processing program Percolator (v1.2) [35, 36] for statistical validation, with a 1% *q*-value (FDR) and peptide significance threshold of 5% (PEP, 0.05). All significant peptides were assigned to protein groups based on the principle of parsimonious analysis [37] and all peptides labeled as unique or duplicate along with their status (*i.e.*, razor, unique or degenerate).

SignalP 4.0 [38] and SecretomeP 2.0 [39] algorithms (Center for Biological Sequence Analysis) were used to predict classical and non-classical secretion modes, respectively. A SecretomeP score >0.5 indicates a high probability of secretion via a non-classical pathway. Transmembrane prediction based on a Hidden Markov model was performed using TMHMM 2.0 (www.cbs.dtu.dk/services/TMHMM/) [40]. The MEROPS peptidase database (http://merops.sanger.ac.uk/) was used as resources for annotating proteolytic events and determining substrate specificity [41]. Raw mass spectrometry data is deposited in the PeptideAtlas and can be accessed at http://www.peptideatlas.org/PASS/PASS00258 [42-44].

Label-free spectral counting – The relative abundance of a protein within a sample was estimated using semi-quantitative normalized spectral count ratios (N_{SC}). For each individual protein, the number of significant (*q*-value <0.01) scoring peptide spectra matches (PSMs) were summed, and normalized by the total number of significant scoring PSMs in the sample (Eqn.1) [33, 45].

$$N_{SC} = (n+f)/[t-(n+f)] \qquad \text{Eqn. 1}$$

where *n* is the number of significant PSMs for each protein in the sample, *t* is the total number of significant PSMs in the sample and *f* is the correction factor set to 1.25 (this factor allows relative quantitation of all proteins within both normalized datasets to be performed).

To compare relative protein abundance between samples the ratio of normalized spectral counts (R_{SC}) was estimated (Eqn. 2), as previously described [33, 46].

$$R_{SC} = [(n_{SUL}+f)\ [t_{CON}-(n_{CON}+f)]\ /\ (n_{CON}+f)\ [t_{SUL}-(n_{SUL}+f)]] \qquad \text{Eqn. 2}$$

where *n* is the number of significant PSMs, *t* is the total number of significant PSMs, *f* is a correction factor set to 1.25, and *CON* (control) and *SUL* (sulindac). The number of significant assigned spectra for each protein was used to determine whether the protein was differentially expressed between the two categories (control and sulindac-treated). For each protein the Fisher's Exact test was applied to significant assigned spectral values. The resulting p-values were corrected for multiple testing using the Benjamini-Hochberg procedure [47]. Our protein list represents those that remained significant at the 0.05 level after this correction, with computation analyses performed using R [48].

Label-free peptide total ion current (TIC) – In addition to label-free spectral counting, the TIC of identified peptides is reported. Asara *et al*., [49] have shown that the TIC has advantages over simple spectral counting including increased dynamic range and quantification for low spectral counts.

Western blot analysis - LIM1215 cell were treated with normal RPMI 1640 media with 1.5 M Tris-HCl, or RPMI-1640 media with 1 mM sulindac (4, 8, 10, 12, 16, 24 h) to analyze cellular and secretome protein expression. Cell lysis was obtained by washing cells twice with ice-cold PBS (10 mL) and lysed with 2 mL of 2 × SDS sample buffer (4% (w/v) SDS, 20% (v/v) glycerol and 0.01% (v/v) bromophenol blue, 0.125 M Tris-HCl, pH 6.8) for 10 min on ice, followed by centrifugation (400,000 × g, 30 min) (TLA-100.2 rotor, Beckman) to remove insoluble material. Cell lysate (30 µg) and secretome samples (10 µg) were lysed in SDS sample buffer and reduced with 50 mM DTT (when required), heated for 5 min at 95 °C and subjected to electrophoresis using precast NuPAGE™ 4-12% (w/v) Bis-Tris Precast gels (Invitrogen) in MES running buffer at a constant 150 V for 1 h. Proteins were electrotransferred onto nitrocellulose membranes using the iBlot™ Dry Blotting System (Invitrogen) and the membranes blocked with 5% (w/v) skim milk powder in Tris-buffered saline (TBS; 50 mM Tris, 150 mM NaCl) with 0.05% (v/v) Tween-20 (TTBS) for 1 h. Membranes were probed with primary mouse anti-E-cadherin (BD Biosciences) (1:2500), rabbit anti-laminin $\gamma 1$ (Abcam, Cambridge, UK) (1:1000), mouse anti-Cab45 antibody (BD Biosciences) (1:1000), rabbit anti-MMP-1 (Santa Cruz Biotechnology) (1:1000), mouse anti-FAK (BD Biosciences) (1:4000), mouse anti-FAK Tyr^{397} (BD Biosciences) (1:4000), for 1 h in TTBS, followed by secondary antibody incubation; HRP conjugated anti-rabbit, anti-goat or anti-mouse antibodies (1:5000) (BioRad Life Sciences), or goat anti-rabbit IgG IRDye 680 (1:5000) (LI-COR Biosciences). Antigen-antibody complex detection was performed using an Odyssey Infrared Imaging System, v3.0 (LI-COR Biosciences, Nebraska USA). Loading controls were obtained by subsequent Deep Purple™ Total Protein staining (GE Healthcare) of membranes following Western blotting.

RESULTS and DISCUSSION

The use of the NSAID sulindac has been attributed to inhibitory effects on tumour growth in gastric, breast, lung, and CRC in nude mice, resulting in a decrease in cell growth and increased apoptosis [50-53]. Although studies have been performed on the chemopreventive actions of sulindac and its metabolites in these systems, the underlying mechanisms of action, especially events associated with apoptotic-onset, are still poorly understood. As a first step toward understanding NSAID-mediated anticancer activity in the context of the tumour environment, we have used the human colon carcinoma cell line LIM1215 to monitor the effect of sulindac on secretome and secretopeptidome (<3 kDa) expression levels.

Sulindac metabolism - Sulindac is a pro-drug, containing a methyl sulfoxide group, which must be reduced to sulindac sulfide to be active as a COX inhibitor [54]. Previous results indicate that the reduction of (S)-sulindac to sulindac sulfide, the active NSAID, is catalyzed by methionine sulfoxide reductase (Msr) A [55, 56]. The Msr family of enzymes (MsrA and MsrB classes) are primarily responsible for the reduction of protein-bound methionine sulfoxide to methionine and play an important role in protecting cells against oxidative damage and aging [57]. Based on cancer tissue expression from the Human Protein Atlas database [58] most colon carcinoma tissues express MsrA and MsrB1/2 at moderate straining levels. Because MsrA is a potentially secreted protein, based on Swiss-Prot and Human Protein Atlas, it is possible that sulindac applied within the LIM1215 culture medium in this study can be metabolised by cell-secreted MsrA. In this study we cannot speculate on the level of sulindac metabolism (sulindac sulphide conversion) in this model without further experimentation.

Assessment of early-onset stage of apoptosis in LIM1215 cells by sulindac

In order to perform MS-based proteome analyses on proteins/peptides released from cancer cells grown *in vitro* it is important to develop cell culture conditions using serum-free media (SFM) otherwise the high concentration of albumin in FCS will compromise MS-based protein identifications. Cell proliferation and viability of LIM1215 cells cultured using SFM over 24 h was ~95-97 % based on MTT assay and trypan blue staining (data not shown), which is in accordance with our previous study [26]. Under serum-free medium conditions LIM1215 cell proliferation was inhibited in a dose-dependent manner in response to 1 mM sulindac treatment (Fig. 1A). Live-cell imaging of LIM1215 cells cultured in SFM containing propidium iodide (PI) was used to monitor changes in cell morphology and membrane integrity [59] (Fig. 1B, Supplemental Video 1). It can be seen that following 12 h sulindac exposure cell detachment and loss of cell membrane integrity was apparent. To further assess early-stage onset of apoptosis, Annexin V-FITC binding assay [60] revealed increased binding to phoshatidylserine following 8 h treatment with 1 mM sulindac (Fig. 2A). Consistent with this finding was the observed phosphorylation change in focal adhesion kinase (FAK). Although there was no significant reduction in FAK expression levels following sulindac treatment, FAK activity (evidenced by tyrosine phosphorylation of FAK-Tyr^{397} [61]) diminished appreciably (Fig. 2B). FAK is activated and localized at FAs upon cell adhesion to the ECM through integrin binding, triggering phosphorylation of FAK-Tyr^{397}. Hypophosphorylation of FAK-Tyr^{397} results in proteolytic degradation of FAK, inhibiting kinase activity, and modulating cell migration and adhesion [62]. Our data agrees with previous reports of NSAIDs, including sulindac, modulating FA architecture through FAK and sensitivity to apoptosis through cell-detachment (*i.e.*, anoikis) [63]. Sulindac sulfide has been shown to modulate apoptosis by integrin-mediated signaling through dephosphorylation of FAK in sporadic and heritable CRC [64].

To further establish the time of onset of apoptosis in response to 1 mM sulindac, cleavage and activation of caspase-3 was monitored by Western blotting (Fig. 2C). Cleavage of pro-caspase-3 (32 kDa) into active caspase-3 fragments (17–10 kDa) was observed following 16 h sulindac treatment. Taken together, these findings establish that 1 mM sulindac induces LIM1215 cell detachment and loss of cell membrane integrity from 12 h, and apoptosis following 16 h. For these reasons conditions where LIM1215 cells were treated with 1 mM sulindac for 8 h were chosen to study early changes in secretome before the onset of apoptosis.

Isolation and characterization of the secretome

The strategy to investigate the LIM1215 secretome (8 h treatment with 1 mM sulindac) is shown in Fig. 3. In total 9,029 peptides were identified from 987 proteins using a stringency of two or more identified peptides for each protein (Supplemental Table 1); 891 proteins (6,601 peptides) and 883 proteins (6,848 peptides) from sulindac-treated and untreated secretomes, respectively, with an overlap of 788 proteins (Supplemental Figure 1A). A comparison of identified proteins between the secretome (bottom-up proteomics methodology) and secretopeptidome (top-down, intact) analyses were performed. For sulindac treated, a total of 896 proteins (7607 peptides) were identified in the >30K fraction, 205 proteins (760 peptides) identified in the 3-30K fraction, while 149 proteins (578 peptides) identified in 1-3K secretopeptidome fraction (Supplemental Figure 1B). A total of 41 proteins were identified common to each of these preparations, while 23 proteins were unique to the secretopeptidome fraction. In comparison, for the control, a total of 869 proteins (7701 peptides) were identified in the >30K fraction, 145 proteins (760 peptides) identified in the 3-30K fraction, while 168 proteins (508 peptides) identified in 1-3K secretopeptidome fraction (Supplemental Figure 3C). A total of 34 proteins were identified common to each of these preparations, while 27 proteins were unique to the secretopeptidome fraction. A comparison between the conventional bottom-up proteomics approach and the peptidomic top-down approach revealed distinct variations for each analysis approach (Supplemental Figure 1B/C, Supplemental Table 1).

Based on UniProt annotation, of the 987 proteins identified, 144 (14.6%) proteins were classified as secreted, extracellular, or cell membrane-derived and 80 proteins predicted to contain at least one transmembrane-spanning domain based upon Kyte-Doolittle hydropathy scores [65]. Using SignalP 4.0 [38] and SecretomeP 2.0 [39] algorithms, a total of 656 proteins (66.5%) were categorized as being secreted by classical and non-classical means (Table 1): 189 proteins predicted by SignalP to be classically secreted, 467 proteins predicted to be non-classically secreted based on SignalP and SecretomeP (<0.5).

To determine the relative abundance of proteins within samples, two different approaches were used based on analysis type: label-free spectral counting (Rsc) for combined identified peptides from all datasets (1-3K, 3-30K and >30K fractions) and label-free precursor ion intensity (total ion counts, sTIC) for endogenous peptides in the RP-HPLC separated 1-3K fractions. For label-free spectral counting, the total number of significant peptide spectra identified for each protein was summed and normalized by the total number of significant peptide spectral counts in the sample (see Eqn. 1 in Experimental Procedures). To compare relative protein abundance between samples the ratio of normalized spectral counts (R_{SC}) was calculated using Eqn. 2 [33]. Thus, a higher normalized spectral count ratio (N_{SC}) reflects higher protein abundance. For all identified proteins, adjusted p-values, as well as confidence limits are shown in Supplemental Table 1. An annotated Volcano plot of adjusted p-values and normalized spectral counts ratio's shows which proteins are significantly up- or down-regulated (Supplemental Figure 2). Based on R_{SC} ratios (Supplemental Table 1), the expression level of collagen alpha-1(XII) chain (R_{SC} -46.9) was the most decreased protein in the sulindac-secretome, relative to the untreated sample (control). While spectral count quantitation provides an accurate estimation for high-abundance proteins, it is limited in its ability to quantify low abundance species (<10 kDa) with low spectral counts [49, 66]. For these reasons we utilized label-free precursor ion intensity to analyze the peptidome (1-3K fractions).

Sulindac attenuates expression of components involved in cell-cell adhesion

Proteomic profiling of the sulindac secretome revealed a diminution of expression levels of many components involved in cell-cell adhesion, including cadherins, desmosomes, and integrins (Table 2). For example, the expression level of protocadherin Fat1 was significantly attenuated (R_{SC} -5.0) – protocadherin Fat1 (FAT1) is a member of integral membrane proteins that regulate cell growth, cell–cell connectivity, gene expression, and planar cell polarity and functions as an adhesion/signaling receptor [67]. This is the first report of FAT1 with relevance to NSAID activity. FAT1 has been suggested to act as a receptor that transduces extracellular cues [68], however the association and function of FAT1 with the tumor microenvironment has not yet been defined. Diminished expression of Lactadherin (R_{SC} -4.2), important in maintenance of intestinal epithelial homeostasis and promotion of mucosal healing [69], Cell adhesion molecule 1 (R_{SC} -1.5), and Desmocollin 2 (R_{SC} -2.3), which functions in maintenance of tissue integrity and architecture [70] were observed following sulindac exposure (Table 2). Lactadherin has been shown to regulate cyclins D1/D3 expression and enhance the tumorigenic potential of mammary epithelial cells [71], while molecular mechanisms responsible for altered Desmocollin 2 expression are not known. This study represents the first report of either Lactadherin or Desmocollin 2 associated with NSAID activity. Further, Cell adhesion molecule 1 (CADM1), a key modulator of the microenvironment to sensitize tumor cells to immune-surveillance [72], has not been described associated with activity of NSAIDs. Similarly, members of the integrin cell surface receptor family were dysregulated following sulindac exposure for 8 h, including ITGA2 (R_{SC} 1.2), ITGA3 (R_{SC} -1.6), ITGA6 (R_{SC} 1.6), and ITGB1 (R_{SC} 4.1). Recent findings have attributed integrins to be directly modulated by chemopreventive agents, including sulindac, to modulate induction of apoptosis through loss of cell-detachment [64]. These findings highlight the importance of the secretome and associated changes to cell-cell adhesion prior to the onset of apoptosis.

Sulindac modulates remodeling of extracellular matrix components

Expression levels of secreted proteins associated with the ECM were shown to be significantly attenuated in response to sulindac – these include collagens, proteoglycans, adhesive glycoproteins, matricellular components, and various proteases (Table 2). Foremost amongst these were collagens (COL12A1, R_{SC} -46.9; COL4A2, R_{SC} -3.4), and the basement membrane laminin receptors (LAMA3, R_{SC} -5.8; LAMA5, R_{SC} -7.3; LAMB1, R_{SC} -22.7; LAMB2, R_{SC} -7.4; LAMB3, R_{SC} -3.4; LAMC1, R_{SC} -8.6; LAMC2, R_{SC} -4.2). Confocal immuno-fluorescence and western blotting of laminin-γ1 (LAMC1) confirmed the diminution in response to sulindac treatment based on semi-quantitative label-free spectral counting (Fig. 4A/B/C). Laminins are key epithelial-derived ECM components of the basement membrane that underlie intestinal epithelial cells [73]. Interestingly, in glioblastoma cells NSAIDs have been shown to down-regulate gene and protein expression of laminin γ1 resulting in attenuated tumor invasion capability [74]. Laminins form independent networks with type IV collagen through proteoglycans, and interact with the cell membranes through integrins and other cell membrane receptors, including dystroglycan. In this study several proteoglycans were identified, including chondroitin sulfate proteoglycan 4 (CSPG4, R_{SC} 2.6), glypicans -1 and -4 (GPC1, R_{SC} -6.8; GPC4, R_{SC} -2.3) and perlecan (HSPG2, R_{SC} -8.0). Consistent with these findings, many NSAIDs limit the expression and activity of proteoglycans [75, 76]. These data suggest that sulindac modulates the expression of key ECM components collagens, laminins, and proteoglycans prior to the onset of apoptosis.

An interesting finding was spatio-temporal localization of E-cadherin in LIM1215 cells upon sulindac treatment. While no change in the expression levels of E-cadherin (CDH1, R_{SC} 1.0) were observed, confocal immuno-fluorescence revealed that in response to sulindac, the subcellular localization of E-cadherin was directed from the plasma membrane (<4 h) to cytosolic expression (from 8 h) (Fig. 4C). This finding is consistent with the observation that sulindac increases intercellular E-cadherin immuno-staining within 48 h in head and neck squamous cell cancer [77].

Proteases and protease inhibitors in the microenvironment play a seminal role in inflammation and cancer [78]. In this study, sulindac was shown to increase the expression levels of proteases associated with the ECM in the LIM1215 cell secretome – many of which are implicated in tissue remodeling, invasion, and metastasis [78-81]. These include matrix metalloproteinase-1 (MMP-1, R_{SC} 5.0) [82], calpain-1 catalytic subunit (R_{SC} 1.6) [83], and ADAM 9 (R_{SC} 1.5) [84] (Table 2). Western immuno-blotting of MMP-1 confirmed the upregulated expression in response to sulindac following 8 h exposure (Fig. 4A/B). Collectively, these findings suggest that early-stage sulindac exposure modulates expression of components throughout the ECM, leading to altered cell-matrix interactions.

Sulindac increases extracellular regulated intramembrane proteolysis (RIP)

In this study although a modest increase in proteolysis was observed in the LIM1215 secretome following treatment with 1 mM sulindac for 8 h, an unexpected finding was enhanced (~40%) regulated intramembrane proteolysis (RIP). RIP describes the proteolytic processing of type I or type II transmembrane proteins, where a membrane-bound ectodomain fragment is subsequently cleaved by I-CliPs into an intracellular domain (ICD) and a soluble, ectodomain [85, 86]. Using a top-down MS analysis strategy (RP-HPLC/ nanoLC-MS/MS) for the 1-3K secretome fraction (peptidome) 33 proteins (from 116 endogenous peptides) were identified in sulindac-treated 1-3K fraction (Supplemental Table 2) compared with 27 proteins (71 peptides) in the control (untreated sample) (Table 3, Supplemental Table 3). However, 21 intramembrane domain fragments (from 8 cell surface protein ectodomains) were identified in the control sample (untreated with sulindac) compared with 53 intramembrane domain fragments (from 17 membrane ectodomains) from sulindac treated secretome samples. These include APP [87], APLP2 [88], SDC1 [89], and epithelial cadherin, CDH1 [90] (Table 3). RIP controls a variety of cellular mechanisms including cellular signaling mediated by several intramembranous cleaving proteases such as the γ-secretases [91]. Interestingly, various

NSAIDs including sulindac and celecoxib have been demonstrated to modulate the activity of membrane-spanning enzymes, including the γ-secretase [92, 93]. These studies suggest an association between NSAIDS and the physical state and fluidity of the PM, activity of γ-secretase, and processing of intramembrane domains.

As an example, extracellular proteolytic peptide fragments from CDH1, a tumor suppressor that facilitates cell-cell adhesion and inhibits migration and invasion [94], were only identified in the sulindac secretome (Fig. 5). CDH1 ectodomain proteolysis has been demonstrated to influence cadherin-mediated adhesion, mediated by ADAM10 [95]. Two peptides were identified, consistent with both ectodomain cleavage and intramembrane proteolysis: ^{701}VEAGLQIPAIL^{711} and ^{698}AQPVEAGLQIPAILG^{712} which is derived from the extracellular/transmembrane CDH1-CTF1$^{701\text{-}882}$ chain. MMP-7 (matrilysin) and MMP-3 (stromelysin-1) have been reported to cleave the ectodomain of CDH1 from both MCF-7 and MDCKts.srcC12 cells, producing a soluble fragment [96]. CDH1 proteolysis and nuclear translocation of the cytoplasmic domain has been attributed to colorectal tumorigenesis [97]. According to the protease and substrate database MEROPS (http://merops.sanger.ac.uk/) [98] ectodomain cleavage of each of the N-terminal CDH1peptides observed in this study are potentially cleaved by various MMPs including MMP-1/2/9/12. Needless to say, further studies are required to determine the functionality of cleaved substrates and peptides, and to establish whether sulindac-induced proteolytic processing of cell surface proteins are associated with a loss in cell adhesion and cell detachment in early-onset stage of apoptosis.

Down-regulated expression of components associated with epithelial mucosal maintenance mediated by sulindac

In addition to their anti-tumor effects, many NSAIDs cause GI ulceration [99]. This damage is caused mainly through the ability of these agents to inhibit prostaglandin synthesis, which has a negative impact on the mucosal maintenance and defense [10]. In this study several secretome components which function in mucosal defense were down-regulated in response to sulindac treatment (Table 4), including glycoprotein-340 (deleted in malignant brain tumors 1, R_{SC} -21.9), mucins 6 (R_{SC} -5.8), 5AC (R_{SC} -4.2), and 13 (R_{SC} -1.1), regenerating islet-derived protein 4 (Reg IV, R_{SC} -3.7), and growth-regulated protein alpha (CXCL1, R_{SC} -5.8). Glycoprotein-340, a secreted glycoprotein and member of the SRCR superfamily, is associated with mucosal defense, cellular immunity and epithelial differentiation [100] and significantly down-regulated during sulindac. Glycoprotein-340 resembles secretory mucins, such as mucin-5AC, in that it contains highly O-glycosylated tandem repeat regions. In the secretome, mucins 6, 5AC, and 13 were down-regulated in expression following sulindac exposure. These mucins are gel-forming glycoproteins of gastric and respiratory tract epithelia [101]. NSAIDs disrupt the production of prostaglandin-E2 which mediates mucin secretion [10]. Similarly, the expression levels of Reg IV, which protects intestinal crypt cells from radiation-induced apoptosis in normal GI tract by modulating GI cell susceptibility [102], were attenuated in LIM1215 secretome by sulindac treatment. This is the first report of these components associated with mucosal maintenance to be modulated by sulindac on human colon tumor cells. The down-regulated expression of these components following sulindac exposure provides important clues into the events associated with adverse *in vivo* effects of several NSAIDs, including sulindac and information towards designing new anti-inflammatory drugs with greater margins of safety.

CONCLUDING REMARKS

In summary, we have developed a protein/peptide separation strategy using differential centrifugal ultrafiltration in combination with 1D-SDS-PAGE/ RP-HPLC and nanoLC-MS-MS to study for the first time the profile of proteins released into the culture (secretome) of LIM1215 cells following treatment with 1 mM sulindac for 8 h. Collectively, our data shows that under these conditions LIM1215 cells secrete decreased levels of proteins associated with extracellular matrix remodeling (e.g., collagens, perlecan, syndecans, filamins, dyneins), cell adhesion (e.g., cadherins, integrins, laminins) and mucosal maintenance (*e.g.*, glycoprotein 340 and mucins 5AC, -6, and 13), while increased expression of various proteases including MMPs and ADAMs. Our results are the first to show enhanced regulated intramembrane proteolysis (RIP) of colon tumor cell surface membrane proteins (e.g., E-cadherin) upon sulindac treatment. Whether or not our *in vitro* secretome findings mediate any of sulindac's growth inhibitory effects *in vivo* is an important area for ongoing studies. A key finding of this study was the diminution of components throughout the secretome associated with mucosal maintenance, which may provide important information towards development of safer anti-inflammatory drugs.

Acknowledgements

Funding was provided by the Australian National Health and Medical Research Council under Program Grant #487922 (RJS). We acknowledge the NHMRC-funded Australian Proteomics Computational Facility (APCF) under Enabling Grant #381413. This work was supported, in part, by funds from the Operational Infrastructure Support Program provided by the Victorian Government, Australia. We acknowledge the Australian Cancer Research Foundation for providing funds to purchase the Orbitrap™ mass spectrometer. We also acknowledge Moshe Olshansky for informatics and statistical analyses.

The authors declare no conflict of interest

References

1. Pisani, P., Bray, F., Parkin, D.M. Estimates of the world-wide prevalence of cancer for 25 sites in the adult population. *Int J Cancer*. **2002**, 97 (1) 72-81.
2. Mann, J.R. and DuBois, R.N. Cyclooxygenase-2 and gastrointestinal cancer. *Cancer J*. **2004**, 10 (3) 145-152.
3. Steinbach, G., Lynch, P.M., Phillips, R.K., Wallace, M.H., Hawk, E., Gordon, G.B., Wakabayashi, N., Saunders, B., Shen, Y., Fujimura, T., Su, L.K. and Levin, B. The effect of celecoxib, a cyclooxygenase-2 inhibitor, in familial adenomatous polyposis. *N Engl J Med*. **2000**, 342 (26) 1946-1952.
4. Gupta, R.A. and Dubois, R.N. Colorectal cancer prevention and treatment by inhibition of cyclooxygenase-2. *Nat Rev Cancer*. **2001**, 1 (1) 11-21.
5. Ulrich, C.M., Bigler, J., Potter, J.D. Non-steroidal anti-inflammatory drugs for cancer prevention: promise, perils and pharmacogenetics. *Nature reviews. Cancer*. **2006**, 6 (2) 130-140.
6. Ruder, E.H., Laiyemo, A.O., Graubard, B.I., Hollenbeck, A.R., Schatzkin, A., Cross, A.J. Non-steroidal anti-inflammatory drugs and colorectal cancer risk in a large, prospective cohort. *The American journal of gastroenterology*. **2011**, 106 (7) 1340-1350.
7. Fischer, S.M., Hawk, E.T., Lubet, R.A. Coxibs and other nonsteroidal anti-inflammatory drugs in animal models of cancer chemoprevention. *Cancer prevention research*. **2011**, 4 (11) 1728-1735.
8. Dube, C., Rostom, A., Lewin, G., Tsertsvadze, A., Barrowman, N., Code, C., Sampson, M., Moher, D. The use of aspirin for primary prevention of colorectal cancer: a systematic review prepared for the U.S. Preventive Services Task Force. *Annals of internal medicine*. **2007**, 146 (5) 365-375.
9. Rostom, A., Dube, C., Lewin, G., Tsertsvadze, A., Barrowman, N., Code, C., Sampson, M., Moher, D. Nonsteroidal anti-inflammatory drugs and cyclooxygenase-2 inhibitors for primary prevention of colorectal cancer: a systematic review prepared for the U.S. Preventive Services Task Force. *Annals of internal medicine*. **2007**, 146 (5) 376-389.
10. Wallace, J.L. Prostaglandins, NSAIDs, and gastric mucosal protection: why doesn't the stomach digest itself? *Physiol Rev*. **2008**, 88 (4) 1547-1565.
11. Sinicrope, F.A., Lemoine, M., Xi, L., Lynch, P.M., Cleary, K.R., Shen, Y., Frazier, M.L. Reduced expression of cyclooxygenase 2 proteins in hereditary nonpolyposis colorectal cancers relative to sporadic cancers. *Gastroenterology*. **1999**, 117 (2) 350-358.
12. Moreira, L. and Castells, A. Cyclooxygenase as a target for colorectal cancer chemoprevention. *Current drug targets*. **2011**, 12 (13) 1888-1894.
13. Danese, S. and Mantovani, A. Inflammatory bowel disease and intestinal cancer: a paradigm of the Yin-Yang interplay between inflammation and cancer. *Oncogene*. **2010**, 29 (23) 3313-3323.
14. Barnes, C.J., Cameron, I.L., Hardman, W.E., Lee, M. Non-steroidol anti-inflammatory drug effect on crypt cell proliferation and apoptosis during initiation of rat colon carcinogenesis. *Br J Cancer*. **1998**, 77 (4) 573-580.
15. Tsujii, M., Kawano, S., Tsuji, S., Sawaoka, H., Hori, M., DuBois, R.N. Cyclooxygenase regulates angiogenesis induced by colon cancer cells. *Cell*. **1998**, 93 (5) 705-716.

16. Rice, P.L., Beard, K.S., Driggers, L.J., Ahnen, D.J. Inhibition of extracellular-signal regulated kinases 1/2 is required for apoptosis of human colon cancer cells in vitro by sulindac metabolites. *Cancer Res*. **2004**, 64 (22) 8148-8151.
17. Grosch, S., Maier, T.J., Schiffmann, S., Geisslinger, G. Cyclooxygenase-2 (COX-2)-independent anticarcinogenic effects of selective COX-2 inhibitors. *J. Natl. Cancer Inst.* **2006**, 98 (11) 736-747.
18. Antonakopoulos, N. and Karamanolis, D.G. The role of NSAIDs in colon cancer prevention. *Hepato-gastroenterology*. **2007**, 54 (78) 1694-1700.
19. Hanahan, D. and Weinberg, R.A. Hallmarks of cancer: the next generation. *Cell*. **2011**, 144 (5) 646-674.
20. Mueller, M.M. and Fusenig, N.E. Friends or foes - bipolar effects of the tumour stroma in cancer. *Nat Rev Cancer*. **2004**, 4 (11) 839-849.
21. Mbeunkui, F. and Johann, D.J., Jr. Cancer and the tumor microenvironment: a review of an essential relationship. *Cancer chemotherapy and pharmacology*. **2009**, 63 (4) 571-582.
22. Bissell, M.J. and Radisky, D. Putting tumours in context. *Nat Rev Cancer*. **2001**, 1 (1) 46-54.
23. Mathivanan, S., Ji, H., Simpson, R.J. Exosomes: Extracellular organelles important in intercellular communication. *J Proteomics*. **2010**, 73 (10) 1907-1920.
24. Albini, A. and Sporn, M.B. The tumour microenvironment as a target for chemoprevention. *Nat Rev Cancer*. **2007**, 7 (2) 139-147.
25. Kenny, P.A., Lee, G.Y., Bissell, M.J. Targeting the tumor microenvironment. *Frontiers in bioscience : a journal and virtual library*. **2007**, 12 3468-3474.
26. Ji, H., Greening, D.W., Kapp, E.A., Moritz, R.L., Simpson, R.J. Secretome-based proteomics reveals sulindac-modulated proteins released from colon cancer cells. *Proteomics Clin. Appl.* **2009**, 3 (4) 433-451.
27. Whitehead, R.H., Macrae, F.A., St John, D.J., Ma, J. A colon cancer cell line (LIM1215) derived from a patient with inherited nonpolyposis colorectal cancer. *J. Natl. Cancer Inst.* **1985**, 74 (4) 759-765.
28. Greening, D.W., Kapp, E.A., Ji, H., Speed, T.P., Simpson, R.J. Colon tumour secretopeptidome: Insights into endogenous proteolytic cleavage events in the colon tumour microenvironment. *Biochim Biophys Acta*. **2013**,
29. Greening, D.W. and Simpson, R.J. 2011. Low-molecular weight plasma proteome analysis using centrifugal ultrafiltration, in Meth. Mol. Biology - Serum/Plasma Proteomics, R.J. Simpson and D.W. Greening, Editors, Springer: New York. p. 109-124.
30. Greening, D.W. and Simpson, R.J. A centrifugal ultrafiltration strategy for isolating the low-molecular weight (</=25K) component of human plasma proteome. *J Proteomics* **2010**, 73 (3) 637-648
31. Steinberg, T.H., Lauber, W.M., Berggren, K., Kemper, C., Yue, S., Patton, W.F. Fluorescence detection of proteins in sodium dodecyl sulfate-polyacrylamide gels using environmentally benign, nonfixative, saline solution. *Electrophoresis*. **2000**, 21 (3) 497-508.
32. Simpson, R.J., Connolly, L.M., Eddes, J.S., Pereira, J.J., Moritz, R.L., Reid, G.E. Proteomic analysis of the human colon carcinoma cell line (LIM 1215): development of a membrane protein database. *Electrophoresis*. **2000**, 21 (9) 1707-1732.
33. Tauro, B.J., Greening, D.W., Mathias, R.A., Ji, H., Mathivanan, S., Scott, A.M., Simpson, R.J. Comparison of ultracentrifugation, density gradient separation, and immunoaffinity capture methods for isolating human colon cancer cell line LIM1863-derived exosomes. *Methods*. **2012**, 56 (2) 293-304.

34. Greening, D.W., Glenister, K.M., Kapp, E.A., Moritz, R.L., Sparrow, R.L., Lynch, G.W., Simpson, R.J. Comparison of human platelet-membrane cytoskeletal proteins with the plasma proteome: Towards understanding the platelet-plasma nexus. *Proteomics Clin. Appl.* **2008**, 2 63-77.
35. Kall, L., Canterbury, J.D., Weston, J., Noble, W.S., MacCoss, M.J. Semi-supervised learning for peptide identification from shotgun proteomics datasets. *Nat Methods*. **2007**, 4 (11) 923-925.
36. Brosch, M., Yu, L., Hubbard, T., Choudhary, J. Accurate and sensitive peptide identification with Mascot Percolator. *J Proteome Res*. **2009**, 8 (6) 3176-3181.
37. Yang, X., Dondeti, V., Dezube, R., Maynard, D.M., Geer, L.Y., Epstein, J., Chen, X., Markey, S.P., Kowalak, J.A. DBParser: web-based software for shotgun proteomic data analyses. *J Proteome Res*. **2004**, 3 (5) 1002-1008.
38. Bendtsen, J.D., Nielsen, H., von Heijne, G., Brunak, S. Improved prediction of signal peptides: SignalP 3.0. *J Mol Biol*. **2004**, 340 (4) 783-795.
39. Bendtsen, J.D., Jensen, L.J., Blom, N., Von Heijne, G., Brunak, S. Feature-based prediction of non-classical and leaderless protein secretion. *Protein Eng Des Sel*. **2004**, 17 (4) 349-356.
40. Krogh, A., Larsson, B., von Heijne, G., Sonnhammer, E.L. Predicting transmembrane protein topology with a hidden Markov model: application to complete genomes. *J Mol Biol*. **2001**, 305 (3) 567-580.
41. Rawlings, N.D., Barrett, A.J., Bateman, A. MEROPS: the database of proteolytic enzymes, their substrates and inhibitors. *Nucleic Acids Res*. **2012**, 40 (Database issue) D343-350.
42. Deutsch, E.W., Lam, H., Aebersold, R. PeptideAtlas: a resource for target selection for emerging targeted proteomics workflows. *EMBO Rep*. **2008**, 9 (5) 429-434.
43. Desiere, F., Deutsch, E.W., King, N.L., Nesvizhskii, A.I., Mallick, P., Eng, J., Chen, S., Eddes, J., Loevenich, S.N., Aebersold, R. The PeptideAtlas project. *Nucleic Acids Res*. **2006**, 34 (Database issue) D655-658.
44. Desiere, F., Deutsch, E.W., Nesvizhskii, A.I., Mallick, P., King, N.L., Eng, J.K., Aderem, A., Boyle, R., Brunner, E., Donohoe, S., Fausto, N., Hafen, E., Hood, L., Katze, M.G., Kennedy, K.A., Kregenow, F., Lee, H., Lin, B., Martin, D., Ranish, J.A., Rawlings, D.J., Samelson, L.E., Shiio, Y., Watts, J.D., Wollscheid, B., Wright, M.E., Yan, W., Yang, L., Yi, E.C., Zhang, H. and Aebersold, R. Integration with the human genome of peptide sequences obtained by high-throughput mass spectrometry. *Genome Biol*. **2005**, 6 (1) R9.
45. Chen, Y.S., Mathias, R.A., Mathivanan, S., Kapp, E.A., Moritz, R.L., Zhu, H.J., Simpson, R.J. Proteomic profiling of MDCK plasma membranes reveals Wnt-5a involvement during oncogenic H-Ras/TGF-{beta}-mediated epithelial-mesenchymal transition. *Mol Cell Proteomics*. **2010**,
46. Old, W.M., Meyer-Arendt, K., Aveline-Wolf, L., Pierce, K.G., Mendoza, A., Sevinsky, J.R., Resing, K.A., Ahn, N.G. Comparison of label-free methods for quantifying human proteins by shotgun proteomics. *Mol Cell Proteomics*. **2005**, 4 (10) 1487-1502.
47. Benjamini, Y. and Hochberg, Y. Controlling the false discovery rate: a practical and powerful approach to multiple testing. *J. R. Stat. Soc. Ser. B-Stat. Methodol.* **1995**, 57 (1) 289-300.
48. Team, R.D.C. 2008. R: A language and environment for statistical computing, in R Foundation for Statistical Computing: Vienna, Austria. p. ISBN 3-900051-900007-900050.

49. Asara, J.M., Christofk, H.R., Freimark, L.M., Cantley, L.C. A label-free quantification method by MS/MS TIC compared to SILAC and spectral counting in a proteomics screen. *Proteomics*. **2008**, 8 (5) 994-999.
50. Fu, S.L., Wu, Y.L., Zhang, Y.P., Qiao, M.M., Chen, Y. Anti-cancer effects of COX-2 inhibitors and their correlation with angiogenesis and invasion in gastric cancer. *World journal of gastroenterology : WJG*. **2004**, 10 (13) 1971-1974.
51. Castonguay, A. and Rioux, N. Inhibition of lung tumourigenesis by sulindac: comparison of two experimental protocols. *Carcinogenesis*. **1997**, 18 (3) 491-496.
52. Sun, B.C., Zhao, X.L., Zhang, S.W., Liu, Y.X., Wang, L., Wang, X. Sulindac induces apoptosis and protects against colon carcinoma in mice. *World journal of gastroenterology : WJG*. **2005**, 11 (18) 2822-2826.
53. Seo, A.M., Hong, S.W., Shin, J.S., Park, I.C., Hong, N.J., Kim, D.J., Lee, W.K., Lee, W.J., Jin, D.H., Lee, M.S. Sulindac induces apoptotic cell death in susceptible human breast cancer cells through, at least in part, inhibition of IKKbeta. *Apoptosis : an international journal on programmed cell death*. **2009**, 14 (7) 913-922.
54. Duggan, D.E., Hooke, K.F., Risley, E.A., Shen, T.Y., Arman, C.G. Identification of the biologically active form of sulindac. *J Pharmacol Exp Ther*. **1977**, 201 (1) 8-13.
55. Moskovitz, J., Weissbach, H., Brot, N. Cloning the expression of a mammalian gene involved in the reduction of methionine sulfoxide residues in proteins. *Proc Natl Acad Sci U S A*. **1996**, 93 (5) 2095-2099.
56. Etienne, F., Resnick, L., Sagher, D., Brot, N., Weissbach, H. Reduction of Sulindac to its active metabolite, sulindac sulfide: assay and role of the methionine sulfoxide reductase system. *Biochem Biophys Res Commun*. **2003**, 312 (4) 1005-1010.
57. Weissbach, H., Resnick, L., Brot, N. Methionine sulfoxide reductases: history and cellular role in protecting against oxidative damage. *Biochim Biophys Acta*. **2005**, 1703 (2) 203-212.
58. Uhlen, M., Bjorling, E., Agaton, C., Szigyarto, C.A., Amini, B., Andersen, E., Andersson, A.C., Angelidou, P., Asplund, A., Asplund, C., Berglund, L., Bergstrom, K., Brumer, H., Cerjan, D., Ekstrom, M., Elobeid, A., Eriksson, C., Fagerberg, L., Falk, R., Fall, J., Forsberg, M., Bjorklund, M.G., Gumbel, K., Halimi, A., Hallin, I., Hamsten, C., Hansson, M., Hedhammar, M., Hercules, G., Kampf, C., Larsson, K., Lindskog, M., Lodewyckx, W., Lund, J., Lundeberg, J., Magnusson, K., Malm, E., Nilsson, P., Odling, J., Oksvold, P., Olsson, I., Oster, E., Ottosson, J., Paavilainen, L., Persson, A., Rimini, R., Rockberg, J., Runeson, M., Sivertsson, A., Skollermo, A., Steen, J., Stenvall, M., Sterky, F., Stromberg, S., Sundberg, M., Tegel, H., Tourle, S., Wahlund, E., Walden, A., Wan, J., Wernerus, H., Westberg, J., Wester, K., Wrethagen, U., Xu, L.L., Hober, S. and Ponten, F. A human protein atlas for normal and cancer tissues based on antibody proteomics. *Molecular & cellular proteomics : MCP*. **2005**, 4 (12) 1920-1932.
59. Vermes, I., Haanen, C., Steffens-Nakken, H., Reutelingsperger, C. A novel assay for apoptosis. Flow cytometric detection of phosphatidylserine expression on early apoptotic cells using fluorescein labelled Annexin V. *Journal of immunological methods*. **1995**, 184 (1) 39-51.
60. Koopman, G., Reutelingsperger, C.P., Kuijten, G.A., Keehnen, R.M., Pals, S.T., van Oers, M.H. Annexin V for flow cytometric detection of phosphatidylserine expression on B cells undergoing apoptosis. *Blood*. **1994**, 84 (5) 1415-1420.
61. Hanks, S.K. and Polte, T.R. Signaling through focal adhesion kinase. *Bioessays*. **1997**, 19 (2) 137-145.

62. Hao, H.F., Naomoto, Y., Bao, X.H., Watanabe, N., Sakurama, K., Noma, K., Tomono, Y., Fukazawa, T., Shirakawa, Y., Yamatsuji, T., Matsuoka, J. and Takaoka, M. Progress in researches about focal adhesion kinase in gastrointestinal tract. *World J Gastroenterol*. **2009**, 15 (47) 5916-5923.
63. Casanova, I., Parreno, M., Farre, L., Guerrero, S., Cespedes, M.V., Pavon, M.A., Sancho, F.J., Marcuello, E., Trias, M., Mangues, R. Celecoxib induces anoikis in human colon carcinoma cells associated with the deregulation of focal adhesions and nuclear translocation of p130Cas. *Int J Cancer*. **2006**, 118 (10) 2381-2389.
64. Weyant, M.J., Carothers, A.M., Bertagnolli, M.E., Bertagnolli, M.M. Colon cancer chemopreventive drugs modulate integrin-mediated signaling pathways. *Clin Cancer Res*. **2000**, 6 (3) 949-956.
65. Kyte, J. and Doolittle, R.F. A simple method for displaying the hydropathic character of a protein. *J Mol Biol*. **1982**, 157 (1) 105-132.
66. Zhu, W., Smith, J.W., Huang, C.M. Mass spectrometry-based label-free quantitative proteomics. *J. Biomed. Biotechnology*. **2010**, 2010 840518.
67. Tanoue, T. and Takeichi, M. Mammalian Fat1 cadherin regulates actin dynamics and cell-cell contact. *J Cell Biol*. **2004**, 165 (4) 517-528.
68. Moeller, M.J., Soofi, A., Braun, G.S., Li, X., Watzl, C., Kriz, W., Holzman, L.B. Protocadherin FAT1 binds Ena/VASP proteins and is necessary for actin dynamics and cell polarization. *Embo J*. **2004**, 23 (19) 3769-3779.
69. Bu, H.F., Zuo, X.L., Wang, X., Ensslin, M.A., Koti, V., Hsueh, W., Raymond, A.S., Shur, B.D., Tan, X.D. Milk fat globule-EGF factor 8/lactadherin plays a crucial role in maintenance and repair of murine intestinal epithelium. *J Clin Invest*. **2007**, 117 (12) 3673-3683.
70. Garrod, D.R., Merritt, A.J., Nie, Z. Desmosomal adhesion: structural basis, molecular mechanism and regulation (Review). *Mol Membr Biol*. **2002**, 19 (2) 81-94.
71. Carrascosa, C., Obula, R.G., Missiaglia, E., Lehr, H.A., Delorenzi, M., Frattini, M., Ruegg, C., Mariotti, A. MFG-E8/lactadherin regulates cyclins D1/D3 expression and enhances the tumorigenic potential of mammary epithelial cells. *Oncogene*. **2012**, 31 (12) 1521-1532.
72. Faraji, F., Pang, Y., Walker, R.C., Nieves Borges, R., Yang, L., Hunter, K.W. Cadm1 is a metastasis susceptibility gene that suppresses metastasis by modifying tumor interaction with the cell-mediated immunity. *PLoS genetics*. **2012**, 8 (9) e1002926.
73. Paez, M.C., Gonzalez, M.J., Serrano, N.C., Shoenfeld, Y., Anaya, J.M. Physiological and pathological implications of laminins: from the gene to the protein. *Autoimmunity*. **2007**, 40 (2) 83-94.
74. Ishibashi, M., Bottone, F.G., Jr., Taniura, S., Kamitani, H., Watanabe, T., Eling, T.E. The cyclooxygenase inhibitor indomethacin modulates gene expression and represses the extracellular matrix protein laminin gamma1 in human glioblastoma cells. *Exp Cell Res*. **2005**, 302 (2) 244-252.
75. Collier, S. and Ghosh, P. Comparison of the effects of non-steroidal anti-inflammatory drugs (NSAIDs) on proteoglycan synthesis by articular cartilage explant and chondrocyte monolayer cultures. *Biochem Pharmacol*. **1991**, 41 (9) 1375-1384.
76. Palmoski, M.J. and Brandt, K.D. Relationship between matrix proteoglycan content and the effects of salicylate and indomethacin on articular cartilage. *Arthritis Rheum*. **1983**, 26 (4) 528-531.
77. Naim, R., Chang, R.C., Schultz, J., Hormann, K. Chemopreventive alteration of the cell-cell adhesion in head and neck squamous cell cancer. *Oncol Rep*. **2006**, 16 (2) 273-277.

78. Sun, J. Matrix metalloproteinases and tissue inhibitor of metalloproteinases are essential for the inflammatory response in cancer cells. *Journal of signal transduction*. **2010**, 2010 985132.
79. Wilkins-Port, C.E., Higgins, S.P., Higgins, C.E., Kobori-Hotchkiss, I., Higgins, P.J. Complex Regulation of the Pericellular Proteolytic Microenvironment during Tumor Progression and Wound Repair: Functional Interactions between the Serine Protease and Matrix Metalloproteinase Cascades. *Biochemistry research international*. **2012**, 2012 454368.
80. van Kempen, L.C., de Visser, K.E., Coussens, L.M. Inflammation, proteases and cancer. *European journal of cancer*. **2006**, 42 (6) 728-734.
81. Joyce, J.A. and Pollard, J.W. Microenvironmental regulation of metastasis. *Nature reviews. Cancer*. **2009**, 9 (4) 239-252.
82. Gupta, G.P., Nguyen, D.X., Chiang, A.C., Bos, P.D., Kim, J.Y., Nadal, C., Gomis, R.R., Manova-Todorova, K., Massague, J. Mediators of vascular remodelling co-opted for sequential steps in lung metastasis. *Nature*. **2007**, 446 (7137) 765-770.
83. Storr, S.J., Carragher, N.O., Frame, M.C., Parr, T., Martin, S.G. The calpain system and cancer. *Nature reviews. Cancer*. **2011**, 11 (5) 364-374.
84. Peduto, L. ADAM9 as a potential target molecule in cancer. *Current pharmaceutical design*. **2009**, 15 (20) 2282-2287.
85. Weihofen, A. and Martoglio, B. Intramembrane-cleaving proteases: controlled liberation of proteins and bioactive peptides. *Trends Cell Biol*. **2003**, 13 (2) 71-78.
86. Lal, M. and Caplan, M. Regulated intramembrane proteolysis: signaling pathways and biological functions. *Physiology*. **2011**, 26 (1) 34-44.
87. Sastre, M., Steiner, H., Fuchs, K., Capell, A., Multhaup, G., Condron, M.M., Teplow, D.B., Haass, C. Presenilin-dependent gamma-secretase processing of beta-amyloid precursor protein at a site corresponding to the S3 cleavage of Notch. *EMBO Rep*. **2001**, 2 (9) 835-841.
88. Hogl, S., Kuhn, P.H., Colombo, A., Lichtenthaler, S.F. Determination of the proteolytic cleavage sites of the amyloid precursor-like protein 2 by the proteases ADAM10, BACE1 and gamma-secretase. *PLoS ONE*. **2011**, 6 (6) e21337.
89. Hemming, M.L., Elias, J.E., Gygi, S.P., Selkoe, D.J. Proteomic profiling of gamma-secretase substrates and mapping of substrate requirements. *PLoS Biol*. **2008**, 6 (10) e257.
90. Marambaud, P., Shioi, J., Serban, G., Georgakopoulos, A., Sarner, S., Nagy, V., Baki, L., Wen, P., Efthimiopoulos, S., Shao, Z., Wisniewski, T. and Robakis, N.K. A presenilin-1/gamma-secretase cleavage releases the E-cadherin intracellular domain and regulates disassembly of adherens junctions. *Embo J*. **2002**, 21 (8) 1948-1956.
91. Brown, M.S., Ye, J., Rawson, R.B., Goldstein, J.L. Regulated intramembrane proteolysis: a control mechanism conserved from bacteria to humans. *Cell*. **2000**, 100 (4) 391-398.
92. Gamerdinger, M., Clement, A.B., Behl, C. Cholesterol-like effects of selective cyclooxygenase inhibitors and fibrates on cellular membranes and amyloid-beta production. *Mol Pharmacol*. **2007**, 72 (1) 141-151.
93. Gamerdinger, M., Clement, A.B., Behl, C. Effects of sulindac sulfide on the membrane architecture and the activity of gamma-secretase. *Neuropharmacology*. **2008**, 54 (6) 998-1005.
94. Nelson, W.J. and Nusse, R. Convergence of Wnt, beta-catenin, and cadherin pathways. *Science*. **2004**, 303 (5663) 1483-1487.
95. Maretzky, T., Reiss, K., Ludwig, A., Buchholz, J., Scholz, F., Proksch, E., de Strooper, B., Hartmann, D., Saftig, P. ADAM10 mediates E-cadherin shedding and regulates epithelial

cell-cell adhesion, migration, and beta-catenin translocation. *Proc Natl Acad Sci U S A*. **2005**, 102 (26) 9182-9187.

96. Noe, V., Fingleton, B., Jacobs, K., Crawford, H.C., Vermeulen, S., Steelant, W., Bruyneel, E., Matrisian, L.M., Mareel, M. Release of an invasion promoter E-cadherin fragment by matrilysin and stromelysin-1. *J Cell Sci*. **2001**, 114 (Pt 1) 111-118.
97. Cespedes, M.V., Larriba, M.J., Pavon, M.A., Alamo, P., Casanova, I., Parreno, M., Feliu, A., Sancho, F.J., Munoz, A., Mangues, R. Site-dependent E-cadherin cleavage and nuclear translocation in a metastatic colorectal cancer model. *American J. Path.* **2010**, 177 (4) 2067-2079.
98. Rawlings, N.D., Barrett, A.J., Bateman, A. MEROPS: the peptidase database. *Nucleic Acids Res*. **2010**, 38 (Database issue) D227-233.
99. Allison, M.C., Howatson, A.G., Torrance, C.J., Lee, F.D., Russell, R.I. Gastrointestinal damage associated with the use of nonsteroidal antiinflammatory drugs. *N Engl J Med*. **1992**, 327 (11) 749-754.
100. Madsen, J., Tornoe, I., Nielsen, O., Lausen, M., Krebs, I., Mollenhauer, J., Kollender, G., Poustka, A., Skjodt, K., Holmskov, U. CRP-ductin, the mouse homologue of gp-340/deleted in malignant brain tumors 1 (DMBT1), binds gram-positive and gram-negative bacteria and interacts with lung surfactant protein D. *Eur J Immunol*. **2003**, 33 (8) 2327-2336.
101. Reid, C.J. and Harris, A. Developmental expression of mucin genes in the human gastrointestinal system. *Gut*. **1998**, 42 (2) 220-226.
102. Bishnupuri, K.S., Luo, Q., Sainathan, S.K., Kikuchi, K., Sureban, S.M., Sabarinathan, M., Gross, J.H., Aden, K., May, R., Houchen, C.W., Anant, S. and Dieckgraefe, B.K. Reg IV regulates normal intestinal and colorectal cancer cell susceptibility to radiation-induced apoptosis. *Gastroenterology*. **2010**, 138 (2) 616-626, 626 e611-612.

Figure Legends & Figures

Figure 1 – Diminished cell proliferation and plasma membrane integrity in LIM1215 cells in response to sulindac. LIM1215 cells were cultured under SFM conditions and treated with vehicle or sulindac (0.2, 0.4, 0.6, 0.8 and 1 mM) for 24 h and proliferation rates determined using MTT assay (A), as described in Experimental Procedures. 1 mM sulindac induced >50% cell inhibition (IC_{50}). Error bars indicating standard deviations are shown for each time point. Values are means of three samples from one of the three independent experiments. Bars, $\pm$SD (n=3, * $P < 0.05$). LIM1215 cells were exposed to 1 mM sulindac containing propidium iodide (PI) for defined periods (0-18 h) and imaged over a 24 h period using Olympus FV1000 confocal system and UPlanSApo 0.9 numerical aperture (NA)/40× objective (B). PI staining (red) and cell detachment (indicated with white arrows) was used to assess plasma membrane integrity, with increased PI staining observed following 12 h exposure to 1 mM sulindac. For time-lapse microscopy refer Supplemental Video 1 with 20 min per frame over the 19 h time-course. Results are representative of three independent experiments.

Figure 2 – Sulindac induces Annexin V binding, loss of focal adhesion and caspase-3 activation in response to sulindac. LIM1215 cells were exposed to vehicle (i, iii, v, vii) or 1 mM sulindac (ii, iv, vi, viii) for defined periods (2, 4, 6, 8 h), and stained for cell apoptosis using Annexin V (white) (A). Apoptosis was evaluated using the TACS™ cell system, as described. Briefly, cells were treated with either vehicle (1.5 mM Tris-HCl, pH 8.5) or 1 mM sulindac, washed with ice-cold PBS, and incubated with Annexin V Incubation Reagent. Cells were subsequently washed in Binding Buffer and viewed using an Olympus FV1000 confocal system and Olympus IX81 microscope. Cells exposed to vehicle showed negligible levels of Annexin V binding for all exposure periods, while sulindac induced Annexin V staining from 8 h (early apoptotic cell formation). Images are

representative of three independent experiments. Expression of FAK and phosphorylation of FAK-Tyr^{397} (activated FAK) was monitored by Western blotting (B). LIM1215 cells were treated with vehicle (1.5 mM Tris-HCl, pH 8.5) or 1 mM sulindac (8 h), and total cellular proteins were prepared as described. Cellular lysates (10 μg) were separated by SDS-PAGE and transferred onto a NC membrane and monitored by Western blotting. Diminished phosphorylation of FAK-Tyr^{397} was observed following 8 h sulindac exposure. Loading controls were obtained by staining the membrane with Deep Purple. The effect of sulindac on caspase-3 cleavage was monitored by Western blotting using an anti-cleaved caspase-3 antibody (17 kDa) following 16 h sulindac incubation (C). LIM1215 cells were treated with vehicle (1.5 mM Tris-HCl, pH 8.5) or 1 mM sulindac (4, 8, 16 h), and whole cell lysates prepared as described. Cell lysates (30 μg) were separated by SDS-PAGE and transferred onto a NC membrane and cleaved caspase-3 detected by Western blotting. Loading controls were obtained by staining the membrane with Deep Purple. Results are representative of three independent experiments.

Figure 3 – Secretome-based proteomic profiling to monitor changes in response to sulindac preceding apoptosis. LIM1215 cells were grown to ∼70% confluence (5×10^7 cells) in RPMI-1640 containing 5% FCS and washed three times with serum-free RPMI. Cells were then allowed to culture in this medium for 24 h. Cells were subsequently treated in presence (1 mM) or absence (control) of sulindac, with the culture medium (CM) collected at 8 h (preceding onset of apoptosis) and centrifuged to obtain the soluble-secretome. Differential centrifugal ultrafiltration (NMWL filters 30K, 3K and 1K) was used to fractionate the soluble-secretome into molecular weight fractions (>30K, 3-30K, 1-3K). Soluble-secreted fractions >30K and 3-30K were analyzed by bottom-up proteomics, where samples were electrophoretically separated using 1D SDS-PAGE and gel bands excised and subjected to reduction, alkylation and trypsinisation. Soluble-secreted fractions 1-3K (*peptidome*) were analyzed by

a top-down proteomic approach, where samples were fractionated using analytical RP-HPLC and concentrated using lyophilisation. Fractions from both proteomic approaches were subsequently analyzed by nanoLC-MS/MS (LTQ-Orbitrap), before database processing and analysis. Identified peptides from the 1-3K fraction were validated using Percolator [35_ENREF_35, 36] with a stringent *q*-value threshold of ≤0.01 and for peptidome analyses, a PEP score ≤0.05.

Figure 4 – Validation of dysregulated extracellular components in response to sulindac revealed during proteomic profiling. Western immuno-blotting of secretome samples (10 μg) confirms reduced levels of laminin-γ1 (A, following 8 h treatment), and elevated Cab45 (A, following 4 h treatment), and MMP-1 (A, following 8 h treatment) in response to sulindac. Deep Purple total protein stain was used as a loading control for all studies. To ascertain the relative abundance of these proteins in the secretome of control and sulindac treated samples (at 8 h), label-free spectral counting was performed (B). For each protein within a sample, the total number of significant tryptic peptide spectra identified for that particular protein was summed and normalized by the total number of significant peptide spectral counts in the sample (see Eqn. 1). A higher normalized spectral count ratio (Rsc) reflects increased protein abundance in that sample. Differentially expressed proteins based on adjusted p-values and normalized spectral counts ratio of laminin-γ1 (LAMC1), Cab45 (SDF4), and MMP-1 (MMP1) are shown. LAMC1 [p-value: $1.518E^{-06}$, Rsc 0.12 (-8.58 negative inverse Rsc)], SDF4 [p-value: $2.88E^{-05}$, Rsc 7.57], and MMP1 [p-value: 0.273, Rsc 4.98] (for upper/lower confidence intervals for these proteins refer Supplemental Table 1). In response to sulindac, expression of laminin-γ1 and E-cadherin was monitored using confocal immuno-fluorescence. Laminin-γ1 expression was shown to decrease from 4 h sulindac treatment, while a change in E-cadherin subcellular localization was observed from the cell membrane (from 4 h) to intracellular compartments (C). Results are representative of three independent experiments.

Figure 5 – Identified peptides from E-cadherin in the peptidome. In response to sulindac increased peptides in the secretome were identified for E-cadherin in the 1-3K dataset. A schematic of human E-cadherin (*P12830*) indicating extracellular (155-709), transmembrane (TM) (710-730), and cytoplasmic (731-882) sequence domains. Identified peptides derived from extracellular/transmembrane domains of E-cad/CTF1 chain are shown. Grey boxes denote peptides derived through proteolysis of extracellular domains (ectodomain cleavage). Ectodomain cleavage sequence analysis indicate E-cad/CTF1 fragments derived through MMP-3/7 proteolysis [96]. Black boxes represent peptides derived through cleavage of intracellular domains (intramembrane proteolysis). Based on sequence analysis proteolysis of these short TM fragments may be the result of presenilin-1/γ-secretase activity.

Figure 1

A

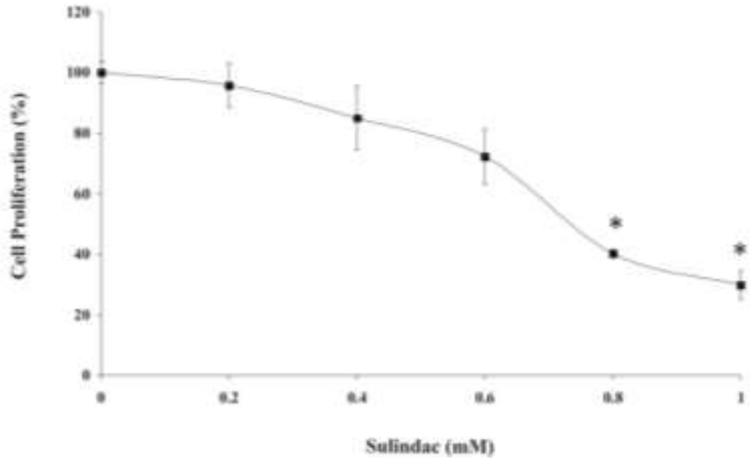
120
100
80
60
40
20
0
Cell Proliferation (%)
*
*
0
0.2
0.4
0.6
0.8
1
Sulindac (mM)

B

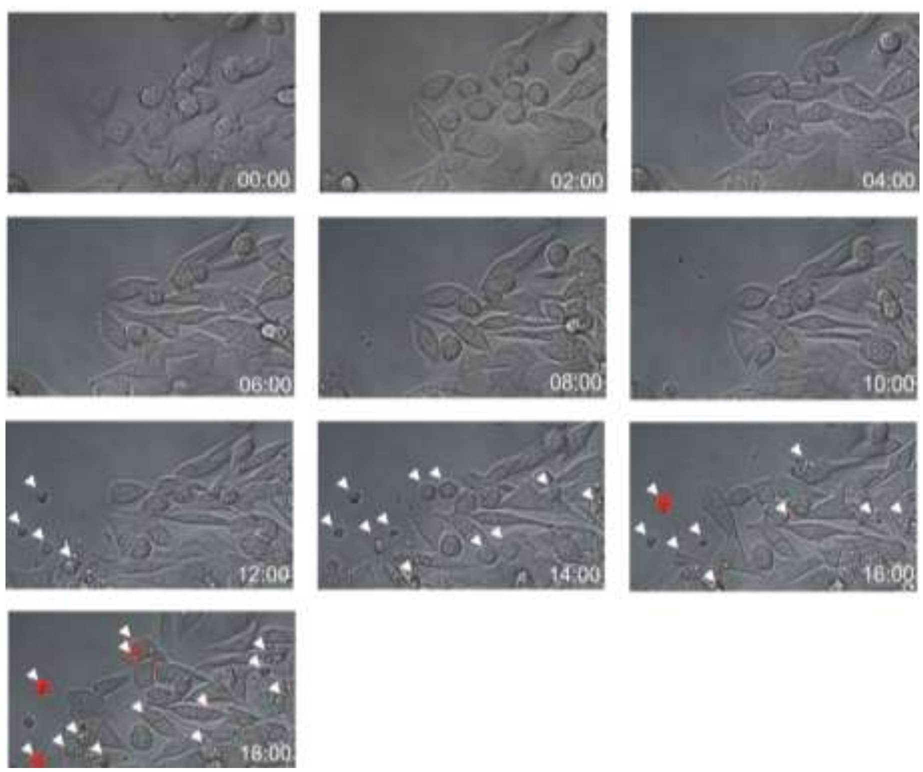
00:00
02:00
04:00
06:00
08:00
10:00
12:00
14:00
16:00
18:00

Figure 2

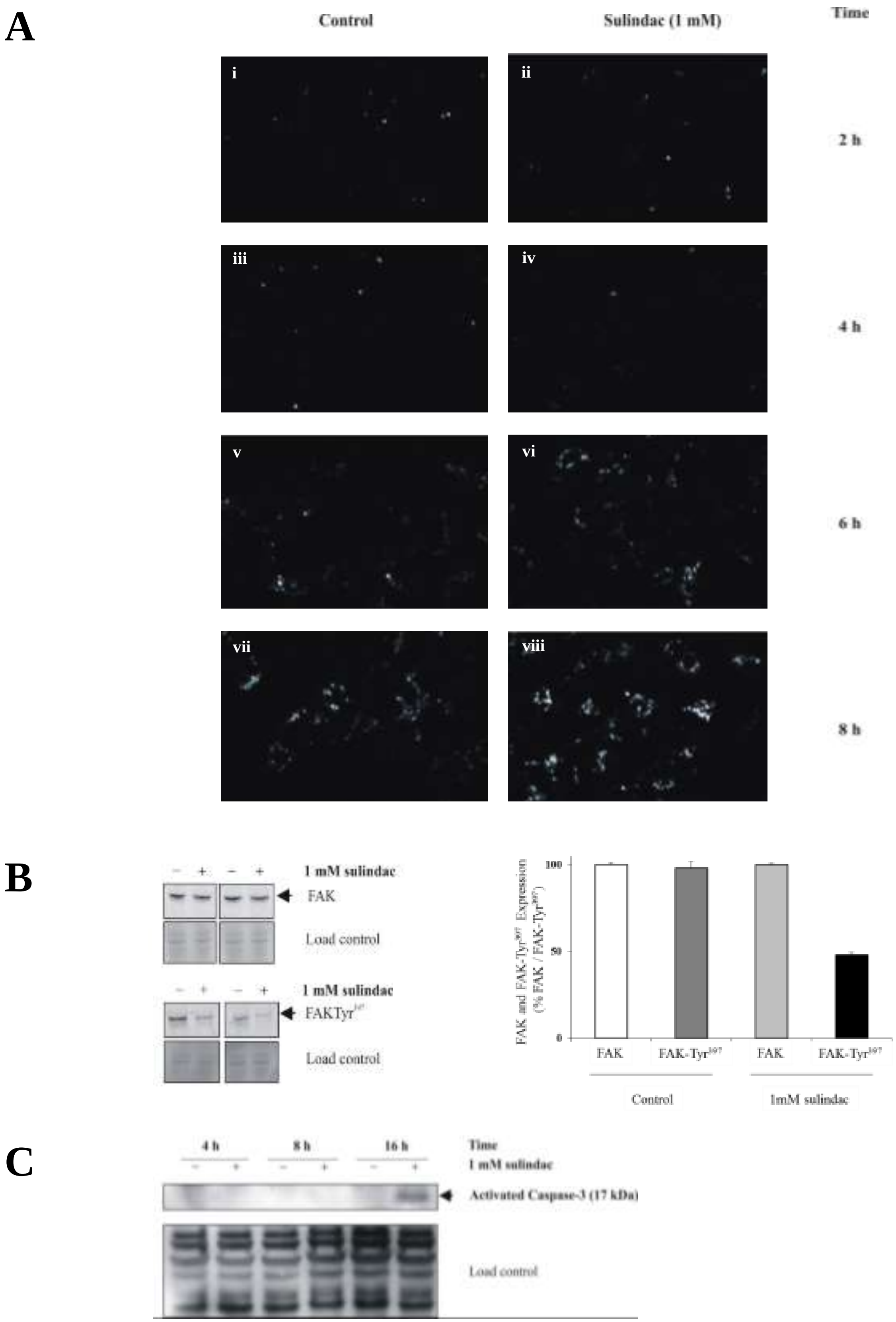
A
Control
Sulindac (1 mM)
Time
i
ii
2 h
iii
iv
4 h
v
vi
6 h
vii
viii
8 h
B
1 mM sulindac
FAK
Load control
1 mM sulindac
FAKTyr397
Load control
FAK and FAK-Tyr397 Expression
(% FAK / FAK-Tyr397)
100
50
0
FAK
FAK-Tyr397
FAK
FAK-Tyr397
Control
1mM sulindac
C
4 h
8 h
16 h
Time
1 mM sulindac
Activated Caspase-3 (17 kDa)
Load control

Figure 3

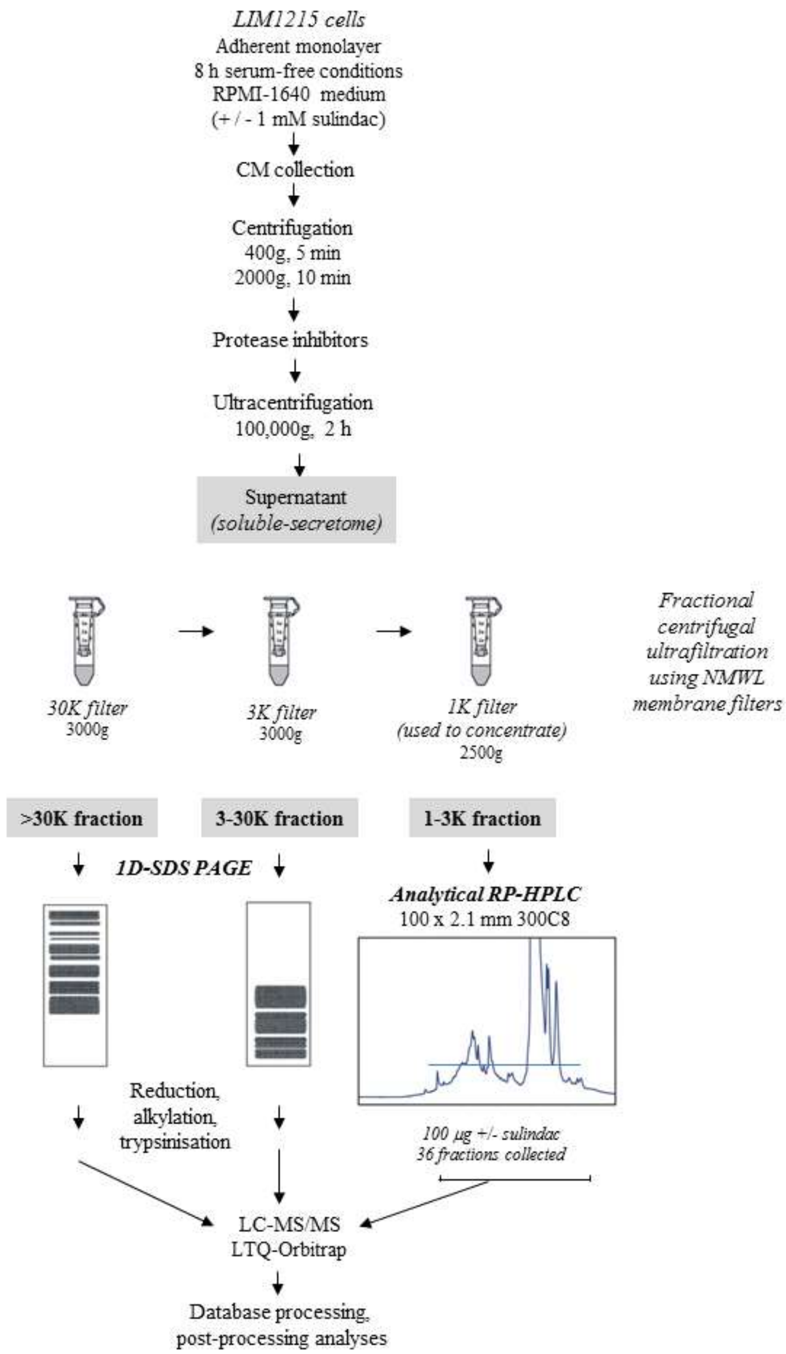
LIM1215 cells
Adherent monolayer
8 h serum-free conditions
RPMI-1640 medium
(+ / - 1 mM sulindac)
CM collection
Centrifugation
400g, 5 min
2000g, 10 min
Protease inhibitors
Ultracentrifugation
100,000g, 2 h
Supernatant
(soluble-secretome)
Fractional centrifugal ultrafiltration using NMWL membrane filters
30K filter
3000g
3K filter
3000g
1K filter
(used to concentrate)
2500g
>30K fraction
3-30K fraction
1-3K fraction
1D-SDS PAGE
Analytical RP-HPLC
100 x 2.1 mm 300C8
Reduction, alkylation, trypsinisation
100 µg +/- sulindac
36 fractions collected
LC-MS/MS
LTQ-Orbitrap
Database processing, post-processing analyses

Figure 4

A

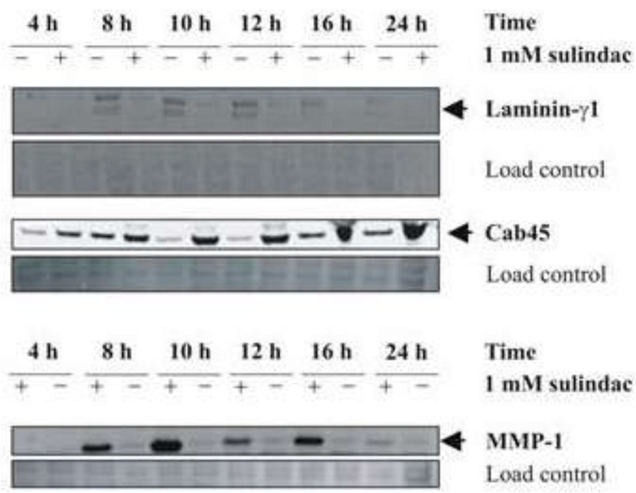
4 h
8 h
10 h
12 h
16 h
24 h
Time
1 mM sulindac
Laminin-γ1
Load control
Cab45
Load control
Time
1 mM sulindac
MMP-1
Load control

B

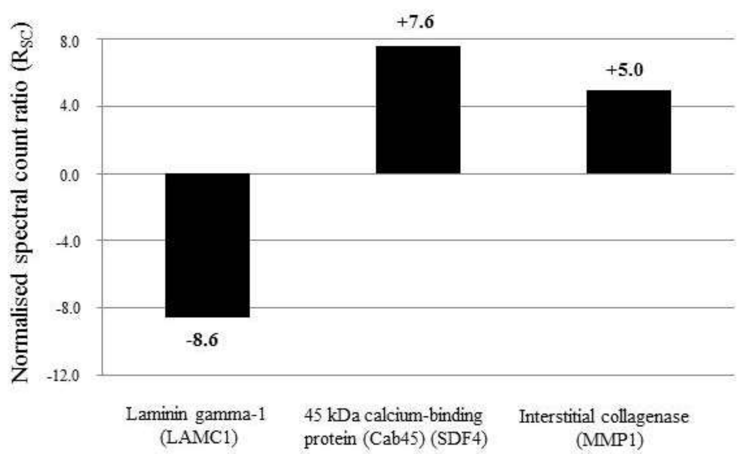
Normalised spectral count ratio (R_{SC})
8.0
4.0
0.0
-4.0
-8.0
-12.0
+7.6
+5.0
-8.6
Laminin gamma-1 (LAMC1)
45 kDa calcium-binding protein (Cab45) (SDF4)
Interstitial collagenase (MMP1)

C

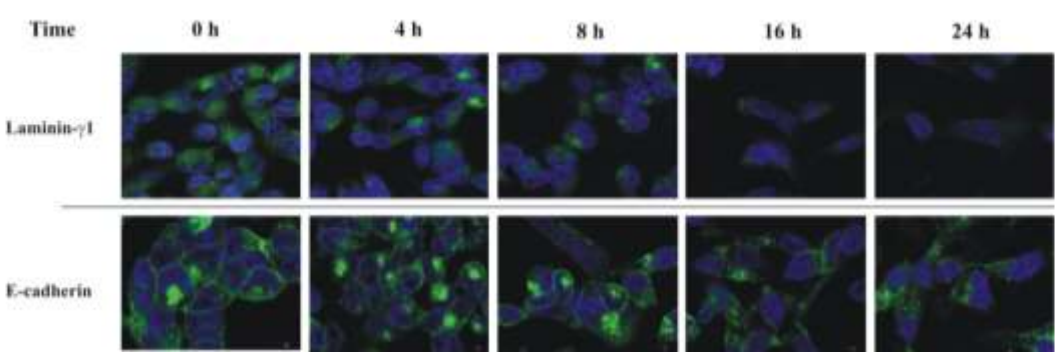
Time
0 h
4 h
8 h
16 h
24 h
Laminin-γ1
E-cadherin

Figure 5

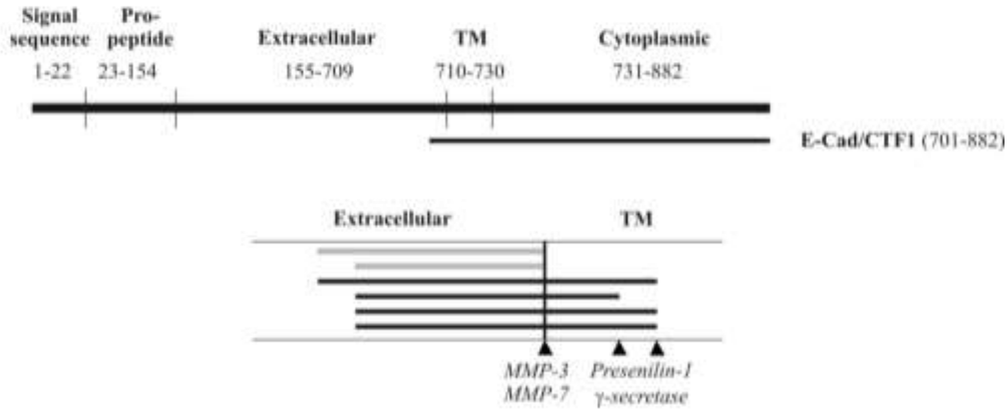

Sequence	Sequence position	Ecto	Rip
(K)AQPVEAGLQIPA(I)	698 - 709		
(P)VEAGLQIPA(I)	701 - 709		
(K)AQPVEAGLQIPAILG(I)	698 - 712		
(P)VEAGLQIPAIL(G)	701 - 711		
(P)VEAGLQIPAILG(I)	701 - 712		
(P)VEAGLQIPAILG(I)	701 - 712		

Table 1 - Predicted protein secretion pathways identified in the control and sulindac secretome

Classical secretion (SignalP)[a]	**Non-classical secretion** (SignalP and SecretomeP)[b]	**Other**[c]	**Predicted secreted** (%)
189	467	331	66.5

a Proteins predicted by SignalP to be classically secreted (SignalP v5.0)

b Proteins predicted to be non-classically secreted using SignalP and SecretomeP (<0.5) (v2.0)

c Proteins not classified as either classically secreted, non-classically secreted, or integral membrane proteins

Refer Supplemental Table 1 for protein information relating to these calculations

Table 2 - *Sulindac modulates remodeling of extracellular matrix and cell-cell adhesion components*

		Acc#[a]	Gene Name	Protein Description	R_{SC}[b]
Cell adhesion components		Q14517 Q08431 O00592 Q9BY67 Q02487 Q16625	FAT1 MFGE8 PODXL CADM1 DSC2 OCLN	Protocadherin Fat 1 Lactadherin Podocalyxin Cell adhesion molecule 1 Desmocollin-2 Occludin	-5.0 -4.2 -3.4 -1.5 -2.3 -2.6
Integrins		P17301 P26006 P23229 P05556	ITGA2 ITGA3 ITGA6 ITGB1	Integrin alpha-2 Integrin alpha-3 Integrin alpha-6 Integrin beta-1	1.2 -1.6 1.6 4.1
Collagens		Q99715 P08572	COL12A1 COL4A2	Collagen alpha-1(XII) chain Collagen alpha-2(IV) chain	-46.9 -3.4
Basement membrane proteoglycans		P98160	HSPG2	Perlecan	-8.1
Proteoglycans and glycosaminoglycans		O00468 Q96S86	AGRN HAPLN3	Agrin Hyaluronan and proteoglycan link protein 3	-4.7 -2.6
Noncollagenous ECM glycoproteins		Q76E14 Q8TDF8 P07942 P55268 Q13751 P11047 Q13753 P07996	LAMA3 LAMA5 LAMB1 LAMB2 LAMB3 LAMC1 LAMC2 THBS1	Laminin alpha 3b chain Laminin alpha5 chain Laminin subunit beta-1 Laminin subunit beta-2 Laminin subunit beta-3 Laminin subunit gamma-1 Laminin subunit gamma-2 Thrombospondin-1	-5.8 -7.3 -22.7 -7.4 -3.4 -8.6 -4.2 -6.9
Structural Matrix		O75413	LTBP4	Latent transforming growth factor beta-binding protein 4	-9.0
Glycan binding		Q08380	LGALS3BP	Galectin-3-binding protein	-2.7
Associated	Syndecans	P18827 P31431	SDC1 SDC4	Syndecan-1 Syndecan-4	-1.8 -2.5
	Cadherins	P12830 Q12864	CDH1 CDH17	Epithelial cadherin (E-cadherin) Cadherin-17	-1.0 -1.5
	Other	Q15582 P07355 P27797 Q14118 P13611	TGFBI ANXA2 CALR DAG1 VCAN	Transforming growth factor-beta-induced protein ig-h3 Annexin A2 Calreticulin (CRP55) Dystroglycan Versican core protein	-2.8 -1.3 2.5 -1.1 -8.2
Proteases		P03956 Q13443 Q9Y5Y6	MMP1 ADAM9 ST14	Interstitial collagenase (Matrix metalloproteinase-1) ADAM 9 Suppressor of tumorigenicity protein 14	5.0 1.5 -1.9

[a] Protein accession from UniProt database, http://www.ebi.uniprot.org/index.shtm.

[b] Relative spectral count ratio (R_{sc}) for proteins identified in treated (1 mM sulindac, 8 h), compared with control (Eqn. 2)

Table 3 – Relative quantification of ectodomain shedding and intramembrane proteolysis in the secreto-peptidome by label-free total peptide ion counts (sTIC)

Acc#[a]	Gene Name	Protein Description	Control peptidome (8 h) *Supplemental Table 2*			Sulindac peptidome (1 mM, 8 h) *Supplemental Table 3*		
			Ion Inten (sTIC)[b]	Extracellular domain peptides #	Intramembrane domain peptides #[d]	Ion Inten (sTIC)[e]	Extracellular domain peptides #	Intramembrane domain peptides #[d]
O14672	ADAM10	Disintegrin and metalloproteinase domain-containing protein 10	35434	3				
Q06481	APLP2	Amyloid-like protein 2	39173	3	1	53830	2	3
P05067	APP	Amyloid beta A4 protein	127693	4	7	97497	2	10
Q9BY67	CADM1	Cell adhesion molecule 1	14985		3	13537		3
P14209	CD99	CD99 antigen	108200	1	2	81391		7
P12830	CDH1	Epithelial cadherin (E-cadherin)	17799			44460	2	4
O95471	CLDN7	Claudin-7				3403	1	
O94985	CLSTN1	Calsyntenin-1	20347	2		40620	1	2
Q14118	DAG1	Dystroglycan				21380		3
P27487	DPP4	Dipeptidyl peptidase 4				49163		1
P98172	EFNB1	Ephrin-B1	33202	1	3	30899	1	3
P16422	EPCAM	Epithelial cell surface antigen	15344		2	7002		2
P21709	EPHA1	Ephrin type-A receptor 1				5513		1
P29317	EPHA2	Ephrin type-A receptor 2				15254		2
P29323	EPHB2	Ephrin type-B receptor 2				25747		3
P54753	EPHB3	Ephrin type-B receptor 3				5099		1
P54760	EPHB4	Ephrin type-B receptor 4				3430	1	
Q99795	GPA33	Cell surface A33 antigen	49641	4		22872	5	
O75144	ICOSLG	ICOS ligand	25566	3				
Q01628	IFITM3	Interferon-induced transmembrane protein 3				17812	2	
P26006	ITGA3	Integrin alpha-3	13710	2				
O75096	LRP4	Low-density lipoprotein receptor-related protein 4	30088	1	1	4548		1
P46531	NOTCH1	Neurogenic locus notch homolog protein 1				10275	1	
O15031	PLXNB2	Plexin-B2	42682	2		68613	2	
Q13308	PTK7	Inactive tyrosine-protein kinase 7				29604	2	1
P10586	PTPRF	Receptor-type tyrosine-protein phosphatase F				11126	2	
Q92692	PVRL2	Poliovirus receptor-related protein 2				19606	2	1
P18827	SDC1	Syndecan-1	41275	4	2	118389	3	6
P31431	SDC4	Syndecan-4	61510	7		36494	6	2
Q9Y5Y6	ST14	Suppressor of tumorigenicity 14 protein	61340	1		12929	2	
O14763	TNFRSF10B	Tumor necrosis factor receptor superfamily member 10B				6772	1	
		Total	**737989**	**38**	**21**	**857265**	**38**	**56**

[a] Protein accession from UniProt database, http://www.ebi.uniprot.org/index.shtm.
[b] Summated total ion current (TIC) for peptides in control with Percolator PEP scores <1% (*q* <0.01)
[c] Number of significant peptides (q <0.01) derived through ectodomain cleavage for control 1-3K
[d] Number of significant peptides (q <0.01) derived through regulated intramembrane proteolysis (within transmembrane domain sequence) for control 1-3K
[e] Summated total ion current (TIC) for peptides in treated (1 mM sulindac, 8 h) with Percolator PEP scores <1% (*q* <0.01)
[f] Number of significant peptides (q <0.01) derived through ectodomain cleavage for treated 1-3K (1 mM sulindac, 8 h)
[g] Number of significant peptides (q <0.01) derived through regulated intramembrane proteolysis (within transmembrane domain sequence) for treated 1-3K (1 mM sulindac, 8 h)

Table 4 - Relative quantification of selected mucosal maintenance & inflammation response proteins dysregulated during sulindac treatment by label-free spectral counting

Acc#[a]	Gene Name	Protein Description	R_{SC}[b]
Q9UGM3	DMBT1	Deleted in malignant brain tumors 1 protein (Glycoprotein 340)	-21.9
O75882	ATRN	Attractin precursor (Mahogany homolog)	-11.4
Q9Y6R7	FCGBP	IgGFc-binding protein precursor (FcgammaBP)	-10.6
Q6W4X9	MUC6	Mucin-6	-5.8
P09341	CXCL1	Growth-regulated protein alpha	-5.8
P98088	MUC5AC	Mucin-5AC	-4.2
Q08431	MFGE8	Lactadherin	-4.2
Q9BYZ8	REG4	Regenerating islet-derived protein 4 precursor (Reg IV)	-3.7
Q9H3R2	MUC13	Mucin-13	-1.1

[a] Protein accession from UniProt database, http://www.ebi.uniprot.org/index.shtm.

[b] Relative spectral count ratio (R_{sc}) for proteins identified in treated (1 mM sulindac, 8 h), compared with control (Eqn. 2)

[c] Details on fold-changes, refer to Supplementary Table I.